AN EXERGY PERSPECTIVE ON SELECTING TECHNICAL PATHWAYS BY WHICH METHANE CAN PROVIDE TRANSPORTATION SERVICES

by

PATRICIA CRANE
B.A.Sc. University of Toronto, 1988

A Thesis Submitted in Partial Fulfillment of the
Requirements for the Degree Of

MASTER OF APPLIED SCIENCE

in the Department of
Mechanical Engineering

We accept this thesis as conforming
to the required standard

[redacted]

Dr. D. S. Scott, Supervisor, Dept. of Mechanical Eng.

[redacted]

Dr. H.-H. Rogner, Member, Dept. of Mechanical Eng.

[redacted]

Dr. R. N. O'Brien, Member, Dept. of Chemistry

[redacted]

Dr. S. Dost, Graduate Advisor, Dept. of Mechanical Eng.

Dr. S. C. Lonergan, External Examiner, Dept. of Geography

Supervisor: Dr. David S. Scott

ABSTRACT

If the premise is accepted that natural gas (and thus methane) will have an increasingly important role as an energy source in the future, then methane must become the chief energy source for the transportation sector. It is also necessary to consider the opportunities for increasingly efficient and low polluting technologies which may arise in the transportation sector. Six candidate pathways are proposed. These involve the energy currencies methanol, methane and hydrogen and the vehicular energy conversion technologies spark ignition engines and solid polymer fuel cells. The energy conversion processes in each pathway are analyzed from two perspectives based on the second law of thermodynamics: efficiency and emission exergy. The theory of exergy analysis is reviewed, and consideration is given to the use of emission exergy as an indicator of potential for environmental impact. All results are normalized based on the energy service transportation, which is defined as one kilometer of city driving. Hydrogen and fuel cell pathways are found to be optimal using these optics.

Examiners:

[redacted]

Dr. D. S. Scott, Supervisor (Dept. of Mechanical Engineering)

[redacted]

Dr. H.-H. Rogner, Member (Dept. of Mechanical Engineering)

[redacted]

Dr. R. N. O'Brien, Outside Member (Dept. of Chemistry)

[redacted]

Dr. S. Dost, Graduate Advisor (Dept. of Mechanical Engineering)

[redacted]

Dr. S. C. Lonergan, External Examiner (Dept. of Geography)

Table of Contents

List of Tables

List of Figures

List of Symbols

COP Coefficient of Performance

$\frac{d}{dt}$ time derivative expressing a rate of accumulation

E total flow exergy of a system

G Gibbs function of a system

g specific Gibbs function of formation

H enthalpy of a system

h specific enthalpy

I irreversibility

n number of moles

p pressure

Q heat

R gas constant

S entropy of a system

s specific entropy

T temperature

V volume

W work

x mole fraction

Subscripts

act actual process

b point on the system boundary at which heat transfer occurs

C cold

e energy

f substance not found in the reference environment

H hot

i point on the system boundary at which mass transfer occurs

k component of a mixture

mix mixture

p product(s)

pdV work due to volume change

ph physical or thermomechanical exergy

r reactant(s)

rev reversible process

ξ exergy

o state of the reference environment

Superscripts

$^{-}$ per mole

$^{\cdot}$ time derivative expressing a flow rate

^{o} concentration in reference environment

Greek Symbols

ϵ specific flow exergy

η efficiency

ι reactant substance

λ product substance

μ chemical potential

ν stoichiometric coefficient

Π entropy production

ψ effectiveness

Acknowledgments

Credit for the highlights of this work primarily belongs to David Sanborn Scott, who is directly responsible for my being in this program, and who has contributed to both my intellectual and spiritual growth over the past two years. I thank him for his inspiration and unfailing encouragement.

Many others were influential in the development and fruition of this thesis. It was my pleasure and privilege to participate in stimulating philosophical and practical discussions with Dr. Web Johnson and Dr. Marc Rosen. As well I would like to thank Dr. Johnson for his work in developing a software package, which ultimately saved me time in determining thermodynamic properties. I greatly appreciate the many helpful suggestions put forth and the enthusiasm shown by Dr. Holger Rogner, Mr. Jean de Grasse, and my fellow graduate students at IESVic: Gary Schubak, Mike Teachman, and John Wells. Dr. Keith Prater of Ballard Power Systems is thanked for generously providing both his time and information about solid polymer fuel cells. Dr. Marianne Scott is recognized for her contribution of wise words and advice, along with Dr. Jim Haddow, for his encouragement and intellectual stimulation. I would also like to thank Dr. Ron Venter, for his guidance in the early days. I am grateful to the people who have ensured that balance remained in my life through camping and hiking trips. I would like to thank my parents and my sister, who have all been very supportive and without whom I would not be here. All of these people deserve recognition for the gems to be found in this thesis. I am responsible for the warts: the assumptions, the places where my ideas become unclear. I can only hope that the reader is able to glean some elements of truth and knowledge from this work.

I would like to recognize the visionaries at Westcoast Energy Inc., who have provided funding for IESVic, without which this project never would have been realized. Finally, I would like to acknowledge the University of Victoria, which has provided funds both for IESVic and Dr. Scott's research, and the B.C.

government, which has also supported me.

Chapter 1

Introduction

1.1 Objectives

The objective of this research is to identify the conditions under which different pathways for the use of methane in the transportation sector, as shown in Figure 1.1, become optimal using the exergy[1] optic.

Figure 1.1 shows the technological routes for methane to enter the transportation sector which are examined in this thesis. Reading from the top down, the first column shows that methane can be converted to methanol, which may then be reformed on-board a vehicle to carbon dioxide and hydrogen. The hydrogen is subsequently used as fuel for a fuel cell stack, which generates dc power and drives a motor, resulting in shaft power to propel a vehicle and provide the energy service transportation. A total of six routes, beginning with methane (the energy source) and ending with the energy service transportation, are investigated.

This analysis applies the exergy method to the various energy transformation processes required along each of the six candidate pathways. There are three subgroups in each pathway: the energy source (methane) to energy currency transformation, the energy currency to energy service transformation, and the exergy of emissions (which may be considered an indicator of potential for

[1] Exergy is defined as the maximum amount of work that can be obtained when a thermodynamic system is brought into equilibrium with the environment.

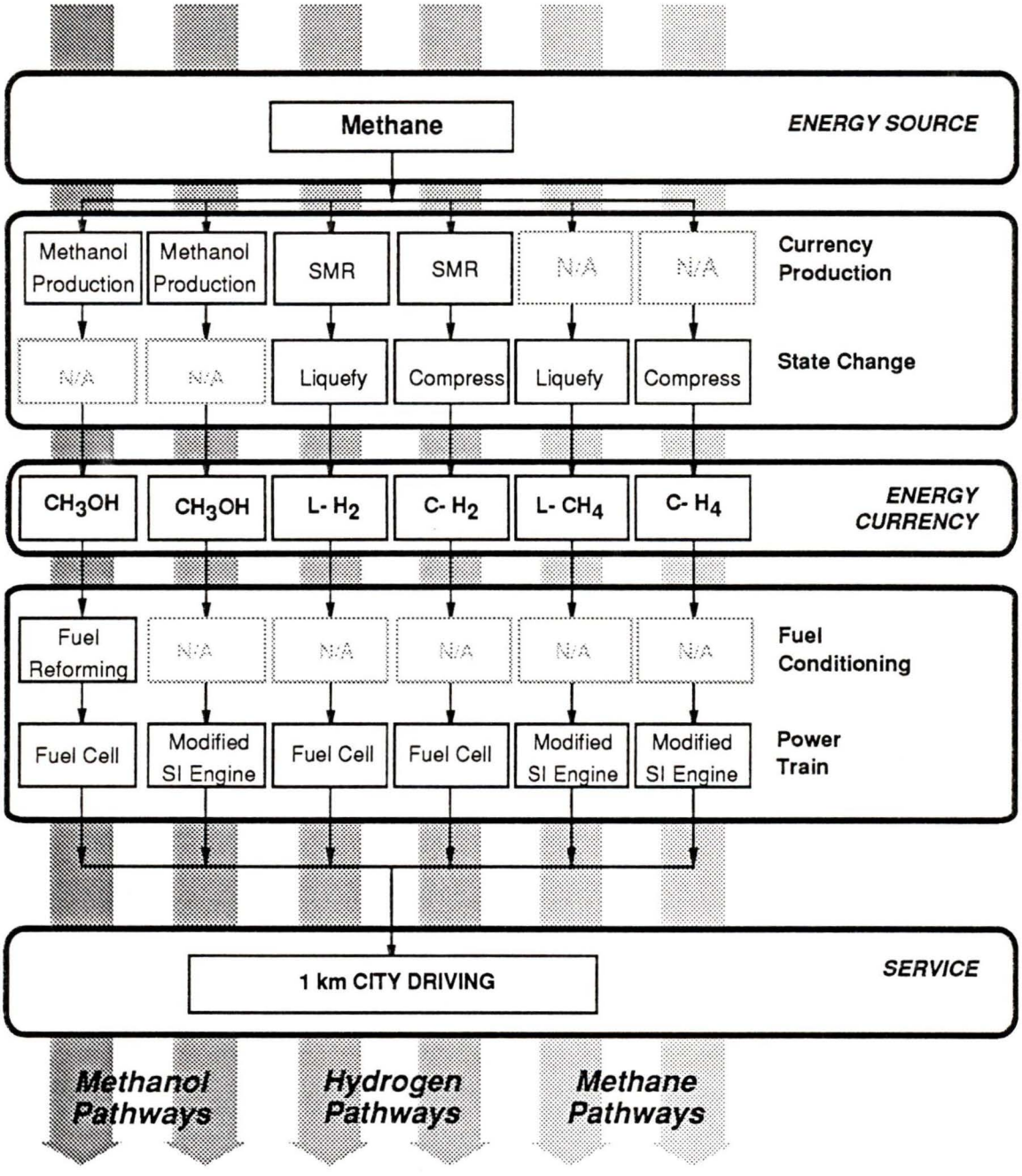

Figure 1.1: Routes for methane to be used in providing the transportation service.

environmental impact). Net exergy efficiency, effectiveness, and exergy of emissions are calculated for each pathway. When inverted, effectiveness can be used to determine the amount of exergy required from the source per unit of service provided. All results are normalized on the basis of transportation service (i.e., per km city driving). This is because the transportation application represents a demand for an energy service, and this service demand acts as a driving force for energy supply. The demand can be filled in a variety of ways, and the idea is to determine which pathway (of those investigated) requires the least exergy input per unit exergy service output. It will also be discovered if the most exergy efficient route corresponds to the route with the lowest potential for environmental impact.

The analysis can be extended to investigate the impact of projected technology improvements (for example, in methane liquefaction) on the pathway affected (in this case, the liquid methane/spark ignition engine route). As well, it can be used to identify those areas which may yield substantial breakthroughs.

1.2 Motivation

Methane is the predominant component of natural gas, accounting for 95% (by volume) of natural gas (as found in a distribution system) [12, 13, 14]. It is anticipated that over the next thirty years natural gas will substantially increase its market share among primary energy sources. An increase in the market share of natural gas can only occur when this energy source makes a significant contribution to the electricity and transportation sectors [15]. This thesis examines the comparative advantages of an array of alternate technical pathways by which methane (and correspondingly natural gas) may enter the transportation sector.

The logistic substitution model, shown in Figure 1.2, arises from the premise that energy sources behave as commodities competing for a share in the mar-

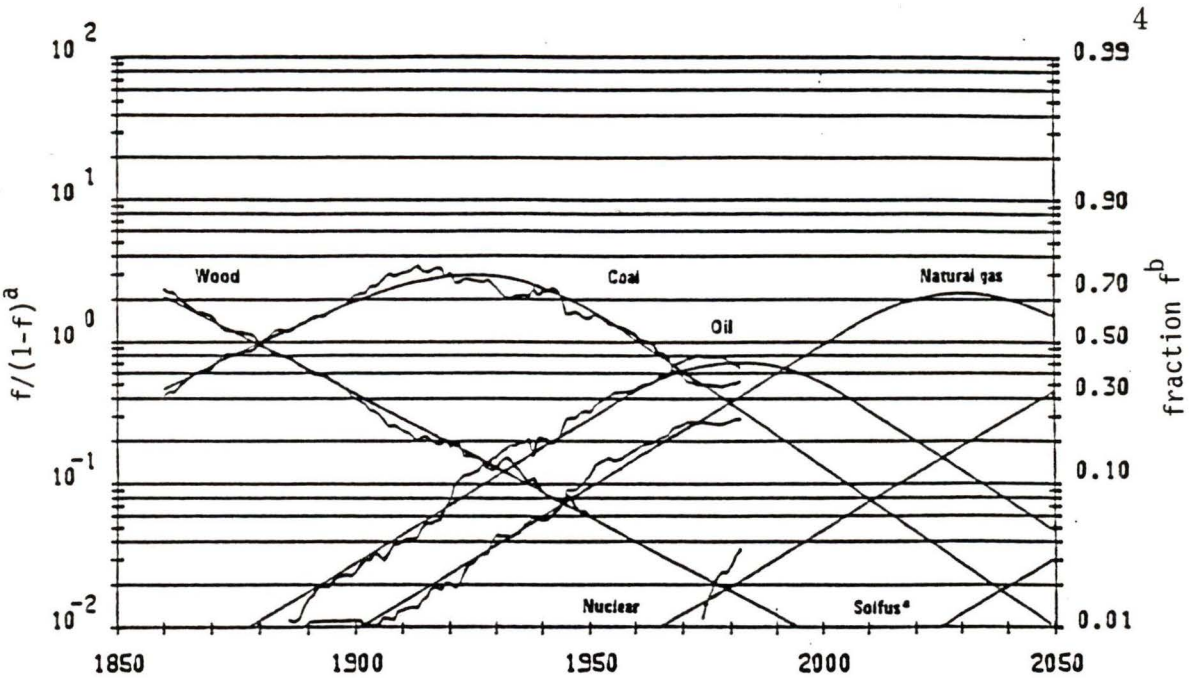

[a] Market share of a technology or primary energy form over the market share not reached by this technology.
[b] f = market share.
[c] Solfus = solar and/or fusion.

Figure 1.2: Market shares of the world's major energy sources from 1860 to 2050: data and the logistic substitution model[2]

[2]From [16].

ketplace. It can be seen historically that the market shares of wood, coal and oil correspond closely to those predicted by the model. The model does not claim to be predictive until a commodity has penetrated the market beyond a few percent[16]. It can be seen that even through times of war and depression, although the actual data may shift off the curve, the model remains quite accurate. The logistic substitution model projects a continued increase in the market share of natural gas for the next four decades, after which its market share stabilizes and then declines as new sources (nuclear, solar, fusion) begin to play more dominant roles. Natural gas appears to be a significant energy source well into the 21^{st} century.

The model shows that coal was used in displacement of wood, oil is being used to displace coal, etc. This substitution comes about as a result of compe-

tition between technologies which are designed for their associated fuels. For example, earlier this century diesel and steam locomotives competed to determine which would power American trains. Diesel won, because the technology was better (better meaning cleaner, more convenient for the operator, etc.) [17]. The technological competition contributed to an increased market share for oil.

It may be recognized that hydrocarbon energy sources entering the market have a higher ratio of hydrogen (H) atoms to carbon (C) atoms than those presently in the market. The H:C ratios of energy sources and energy currencies[3] historically have progressed as in Table 1.1. Coal has an atomic H:C ratio that

Table 1.1: H:C Atomic Ratios in Energy Sources and Currencies[4]

Commodity	Atomic H:C Ratio
Coal	0.7 – 0.9 : 1
Athabasca Oil Sands Bitumen	1.4 – 1.6 : 1
Conventional Crude Oil	1.8 – 1.9 : 1
Liquid Fuels (Gasoline, etc)	2.1 – 2.3 : 1
Natural Gas	$\sim$ 4 : 1

[4]From [18]

is slightly less than one to one, and for crude oil this ratio is greater than one to one. Fuels that are liquid at ambient temperature and pressure (energy currencies such as gasoline, diesel, and Jet A) have atomic H:C ratios of about two to one [18]. Natural gas, with four hydrogen atoms to each carbon atom, has the highest ratio of hydrogen to carbon for a naturally occurring hydrocarbon energy source.

In 1988, the transportation sector was responsible for about 16.8% of the total Canadian primary energy consumption [19]. The energy demands of the

[3]An energy currency is a substance derived from an energy source. It is supplied to the energy consumer who can use it for energy transactions, such as in an energy technology. For example, electricity is an energy currency. It can be derived from coal, oil, sunlight or other sources. It is supplied to users via transmission lines, and its form is readily accepted by light bulbs, microwave ovens, and fax machines.

transportation sector are significant and are primarily met by liquid fuels, because their high energy density on a volume basis allows a vehicle to have a large range with a relatively small fuel tank. Liquid fuels are derived primarily from fossil sources. Incomplete combustion of these fuels in internal combustion engines produces substances which contribute significantly to air pollution and photochemical smog. The other major energy markets (industry and household service) can be readily supplied by gaseous or solid fuels, and by electricity. If natural gas (methane) is to become the principal energy source for the transportation sector, then a high volumetric energy density is desirable for the corresponding energy currencies.

It is generally understood that the emission of carbon dioxide (CO_2) from the combustion of fossil fuels has the potential to greatly contribute to global climatic change. This effect may have dramatic consequences on the planet. As a result, concerned researchers, environmentalists, and the general public have directed the policy makers to introduce legislation promoting clean–burning fuels (that is, fuels releasing little CO_2, sulfur dioxide (SO_2), hydrocarbons, and particulates upon combustion). Methane (CH_4) yields 0.178 kg of CO_2 for every kWh of energy released, as compared to #2 Fuel Oil, which produces 0.251 kg of CO_2 for every kWh of energy released[5]. Reduced CO_2 emissions and virtually zero sulfur content make methane a clean energy alternative.

In the future, following the patterns of market development and considering the environmental drive, methane is expected to become an important energy source in the transportation sector. Methane can be utilized for transportation in a variety of different forms. It may be a feedstock for the production of methanol, other liquid fuels such as diesel, or hydrogen, or it may be used as a fuel itself in a liquid or a compressed state. These options may be compared from the perspective of the second law of thermodynamics, using the thermodynamic

[5]These values were calculated assuming all of the carbon in the fuel to eventually become carbon dioxide, based on 15.43 kWh/kg of CH_4, and 12.40 kWh/kg of #2 Fuel Oil. This data is taken from Chemical Engineering Handbook by Perry, 4th edition, 1969, McGraw Hill.

property exergy. Exergy analysis provides insight into process irreversibilities and indicates where high quality energy is being wasted. Exergy efficiency and emission exergy are two metrics by which different options may be analyzed.

1.3 Methodology

An energy system may be viewed as a chain of energy transformations, from extraction of the energy source from the environment to provision of an energy service, which ultimately returns energy to the environment in some degraded form. Energy sources, such as wood, coal, oil, sunlight and wind, are found as resources in the environment. Technologies transform these sources into energy currencies, such as gasoline, electricity and hydrogen. The energy source to energy currency transformation requires energy, and returns some energy to the environment in the forms of waste heat and combustion gases. The energy currency used to provide an energy service (which may be transportation, communication, or space heating) is chosen to match the energy technology which ultimately provides that service. For example, electricity is used to fuel light bulbs which illuminate the living room. Similarly, Jet A is used to fuel gas turbine engines which ultimately fly passengers from Vancouver to Tokyo.

Several technical pathways (linking energy currencies and energy technologies) exist that will allow the energy source methane to be used in providing the energy service transportation. Methane itself may be the energy currency, used in either liquid or compressed form, for combustion in engines. Alternatively, methane can be processed into methanol (CH_3OH). Methanol can be used in combustion engines or it can be reformed and fed into a fuel cell to create electricity. Hydrogen can also be produced from methane, and can be carried in either liquid or compressed form. It can be most effectively utilized by a fuel cell. The processes which transform energy from a source to a currency themselves require energy. These processes, as well as those which transform energy

in the production of a service, produce low quality energy waste products.

The conversion of methane to methanol, along with all of the energy transformations in the *source to service* chain, are analyzed thermodynamically from the exergy perspective. This is done for all of the pathways in Figure 1.1, examining the dual aspects of efficiency and emissions. Exergy analysis, based on the second law of thermodynamics, provides insight into the quality of energy flows associated with a process. A major difference between the concepts of energy and exergy is that energy is conserved while exergy is not conserved. Exergy analysis is emphasized in this thesis.

It is possible that exergy analysis, which considers the fundamental chemistry of the substances involved, may be used to develop an index to assess the potential environmental impact of waste streams. Szargut [20] has recognized that all waste streams released into the environment, from industrial processes or other sources, possess some exergy, and thus can disturb the equilibrium of the environment. The greater the exergy of the waste stream, the greater the disturbance of the environment. Szargut uses this exergy value as a component in determining a coefficient of ecological cost for any given product.

An appropriate normalization for the exergy of emissions is the service provided. For the purpose of this thesis, the energy service transportation is defined by a city driving schedule, which is implied to be the duty cycle[6] of an automobile. The quantity of exergy input required in order to provide a unit of city driving (i.e., a km of city driving averaged over the duty cycle) is another metric by which to compare the different routes. The analysis is then formed around the energy service. For the purposes of this thesis, it is limited to energy conversion processes. No attempt is made to consider the effects of fuel tank weight on the vehicle, or the energy requirements associated with storage and distribution of the energy currencies.

[6]Duty cycle is used throughout this thesis to mean the load versus time characteristic imposed on a device in order to provide a service.

Chapter 2

Thermodynamic Theory

2.1 Basic Concepts of Exergy Analysis

A brief review of some fundamental concepts and methods in thermodynamics is given here to facilitate the presentation of exergy analysis.

First, it is essential to clearly define the thermodynamic system under consideration. This includes specifying the system boundary with respect to the environment. Unless otherwise specified, the boundary of an open system is permeable to matter, heat, work and fields. The boundary may be real or imaginary. The surroundings consist of everything outside the system, and the environment is a subset of the surroundings such that the environment is large with respect to the system, and may only exchange work of the variety not dependent on volume change with the surroundings. Figure 2.1 shows the system, environment, and surroundings, and the modes by which they interact. Note that heat and mass input to the system are defined as positive and work output from the system is defined as positive. The system plus the environment constitute the combined system, and exergy is defined as the maximum amount of work that can be obtained from the combined system when the system is brought into equilibrium with the environment. Thus exergy is a property of both the system and the environment.

The system is said to be at the restricted dead state when it has reached

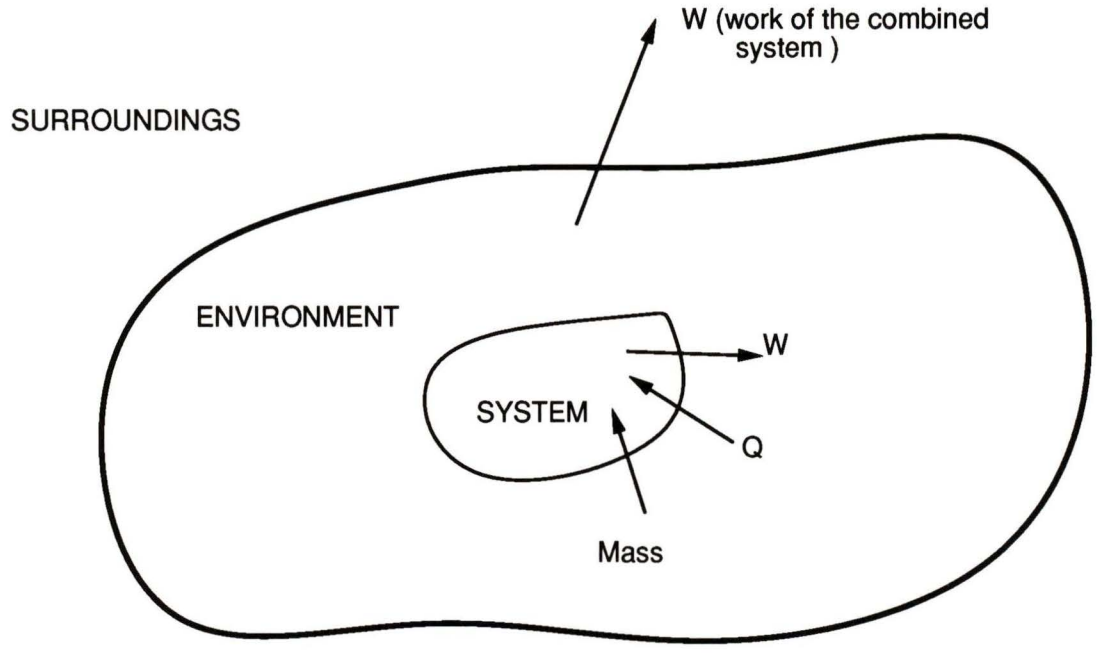

Figure 2.1: Thermodynamic definition of system, environment, and surroundings, and their interactions.

thermomechanical equilibrium with the environment and it is said to be at the dead state when it has reached both thermomechanical and chemical equilibrium with the environment. For this analysis, only simple systems will be examined. This means that gravitational fields, electromagnetic fields, nuclear[1], and surface effects will be neglected. A further simplification is to neglect kinetic energy (and kinetic exergy).

2.1.1 Reference Environment

The reference environment attempts to model the natural, physical environment around the thermodynamic system. It is assumed to be very large in extent, so as to act as a source and a sink for matter and heat. The reference environment

[1]except for hydrogen, H_2, for which the electron spin orientation becomes extremely important as temperature decreases.

is assumed to have constant intensive properties, both spatially and temporally, which indicate an equilibrium state. It consists of common substances found in the atmosphere, hydrosphere, and lithosphere. The reference environment adopted here is based on that of Gaggioli and Petit [21] with the exception that the reference pressure is taken to be 1 bar instead of 1 atmosphere. This is consistent with the 1985 JANAF Thermochemical Property tables [22], from which some thermodynamic data has been obtained. The state and composition of the reference environment used in this thesis is shown in Table 2.1.

Table 2.1: Reference Environment Characteristics[2]

Gaseous Phase	Mole Fraction
N_2	0.7567
O_2	0.2035
H_2O	0.0303
Ar	0.0091
CO_2	0.0003
Other	0.0001
Condensed Phases	
H_2O	liquid
$CaCO_3$	solid
$CaSO_4 \cdot 2H_2O$	solid
$T_o = 298.15$ K	$p_o = 1$ bar

[2]Based on the reference environment in [21]

The reference environment is to some degree subjective. A complete reference environment consists of a stable substance for each element. Ideally, constituents of the reference environment have low Gibbs energy of formation, are found in abundance in the natural environment, and are in stable equilibrium with other reference environment constituents [21].

2.1.2 Exergy Transfer with Mass

Following the method outlined by Moran [23] and the notation of Kotas [24], consider a control volume (open system) consisting of a simple substance. The specific thermomechanical flow exergy (expressed per mole) for a system having a different temperature T and pressure p than the environment (at T_o, p_o) can be expressed as

$$\bar{\epsilon}_{ph} = (\bar{h} - T_o\bar{s}) - (\bar{h}_o - T_o\bar{s}_o) \tag{2.1}$$

where $\bar{h}$ and $\bar{s}$ are the enthalpy and entropy respectively, per mole evaluated at the state of the system (defined by T, p), and $\bar{h}_o$ and $\bar{s}_o$ are evaluated as if the system were at the state of the environment (defined by T_o, p_o). The subscript o denotes the state of the reference environment as defined by its intensive properties, so that the symbol $\bar{h}_o$ indicates the enthalpy per mole of the system in the restricted dead state (T_o, p_o). For an ideal gas mixture,

$$\bar{\epsilon}_{ph,mix} = \sum_k ((\bar{h} - \bar{h_o})_{T,p_k} - T_o(\bar{s} - \bar{s_o})_{T,p_k}) \tag{2.2}$$

Chemical exergy is defined as the maximum amount of work obtainable from the combined system when the system is brought from the restricted dead state to the dead state by processes involving heat and mass transfer only with the environment [24]. The specific chemical exergy of a substance depends on whether or not that substance is found in the reference environment. Substances found in the reference environment undergo an isothermal process from the restricted dead state at T_o, p_o to their final state at $T_o, p_{o,o}$, where $p_{o,o}$ indicates the partial pressure of the substance in the reference environment. Using Dalton's model for ideal gas mixtures, and assuming the system is a mixture of ideal gases, then the partial pressure of the substance in the system is $x_k p_o$, where x_k is the mole fraction of species k in the system, and the partial pressure of the substance in the environment is $x_k^o p_o$, where x_k^o is the mole fraction of species k in the

environment. Thus, the specific chemical exergy, $\bar{\epsilon}_k$, (expressed per mole) of substance k is given by

$$\bar{\epsilon}_{o,k} = \bar{R}T_o \ln\left(\frac{x_k}{x_k^o}\right) \tag{2.3}$$

where $\bar{R}$ is the universal gas constant. The chemical exergy of the entire mixture is simply the sum of the chemical exergies of all of the substances in the mixture. That is,

$$\bar{\epsilon}_{o,mix} = \sum_k x_k \bar{\epsilon}_{o,k} \tag{2.4}$$

If the substance is not found in the reference environment then there is some work which may be developed as it reacts with substances in the reference environment to finally decompose into substances which are found in that environment. For example, if the substance is a fuel such as methane (CH_4), then it will react in the environment as

$$CH_4 + 2O_2 \rightarrow CO_2 + 2H_2O$$

In such a case, the chemical exergy is expressed by

$$\bar{\epsilon}_{o,f} = \bar{g}_{o,f} - \mu_f^o \tag{2.5}$$

where $\bar{g}_{o,f}$ is the Gibbs function of formation for the fuel at T_o and p_o, and

$$\mu_f^o = \sum_p \nu_\lambda \mu_\lambda^o - \sum_r \nu_\iota \mu_\iota^o \tag{2.6}$$

where ν_λ and ν_ι are the stoichiometric coefficients per mole of fuel of the products p and reactants r. Now, if λ and ι are substances in the reference environment, then

$$\mu_\lambda^o = \bar{g}_{o,\lambda} + \bar{R}T_o \ln(x_\lambda^o) \tag{2.7}$$

$$\mu_\iota^o = \bar{g}_{o,\iota} + \bar{R}T_o \ln(x_\iota^o) \tag{2.8}$$

Substituting (2.6), (2.7), and (2.8) into (2.5), it can be shown that

$$\bar{\epsilon}_{o,f} = -\Delta G_o + \bar{R}T_o \left(\sum_r \nu_\iota \ln x_\iota^\circ - \sum_p \nu_\lambda \ln x_\lambda^\circ \right) \tag{2.9}$$

where

$$\Delta G_o = -\bar{g}_{o,f} + \sum_p \nu_\lambda \bar{g}_\lambda - \sum_r \nu_\iota \bar{g}_\iota \tag{2.10}$$

If a substance not found in the reference environment is part of an ideal gas mixture, it is necessary to add the term

$$\bar{R}T_o \ln x_f \tag{2.11}$$

to equation (2.5) to account for the reduced exergy (additional entropy) of the mixture arising from the fact that the substance is part of a mixture (and not a pure substance).

In summary, the exergy transfer with mass includes the thermomechanical exergy of the mass, expressed by (2.1), and the chemical exergy expressed by (2.4) and (2.9). Combining these equations,

$$\dot{n}\bar{\epsilon} = \dot{n}\bar{\epsilon}_{ph,mix} + \sum_f \dot{n}_f(\bar{\epsilon}_{o,f} + \bar{R}T_o \ln x_f) + \sum_k \dot{n}_k \bar{R}T_o \ln(\frac{x_k}{x_k^\circ}) \tag{2.12}$$

where $\dot{n}\bar{\epsilon}$ is the molar flow rate times the specific exergy per mole, i.e., the exergy transfer with mass, $\dot{n}\bar{\epsilon}_{ph,mix}$ is the molar flow rate times the specific physical exergy per unit mole, $\sum_f \dot{n}_f(\bar{\epsilon}_{o,f} + \bar{R}T_o \ln x_f)$ represents the chemical exergy of f substances not found in the reference environment (which includes the reversible work required to compress f substances to their partial pressure in the ideal gas mixture), and $\sum_k \dot{n}_k \bar{R}T_o \ln(\frac{x_k}{x_k^\circ})$ represents the reversible work of compression of k substances in the reference environment to their partial pressures in the ideal gas mixture.

2.1.3 Exergy Transfer with Heat

Consider any system experiencing a heat interaction with it's environment. The rate of exergy transfer associated with a heat transfer, $\dot{\epsilon}^Q$, is defined as

$$\dot{\epsilon}^Q = \dot{Q}(1 - \frac{T_o}{T}) \tag{2.13}$$

where T is the temperature of the system at the boundary where the heat transfer occurs. This is equivalent to the maximum work that an ideal (Carnot) heat engine could produce by operating between the two temperatures. Note that heat at higher temperatures has a higher exergy value than heat at lower temperatures relative to some datum T_o, and for temperatures below T_o, the exergy transfer is in the opposite direction to and may even be greater than the heat transfer.

2.1.4 Exergy Transfer with Work

For the purpose of exergy analysis, work is separated into two types. First there is the work done by a system due to volume change.

$$\dot{W}_{pdv} = \int_{V_1}^{V_2} p d\dot{V} \tag{2.14}$$

where p is the pressure of the system and may be a function of volume and the expression has been formulated on a rate basis. Not all of this work can be used to say, raise a weight. Some work must be done to push back the environment. This amount (over a finite interval) is equal to

$$p_o(V_2 - V_1) \tag{2.15}$$

where p_o is the constant pressure exerted by the environment. Thus the exergy associated with this type of interaction is

$$\dot{E}_{pdv} = \dot{W}_{pdv} - p_o \int_{V_1}^{V_2} d\dot{V} \tag{2.16}$$

A second type of work is known as shaft work. By definition, the exergy associated with shaft work is 100%. It is given the symbol $\dot{W}_x$.

2.1.5 Exergy Destruction

Exergy can not be created, but it may be destroyed. Exergy destruction, also known as irreversibility, is related to entropy production. This relationship is given by the following equation

$$\dot{I} = T_o \dot{\Pi} \tag{2.17}$$

where $\dot{I}$ represents the rate of exergy destruction and $\dot{\Pi}$ represents the rate of entropy production. Irreversibility is the difference between the maximum amount of work that can be obtained from a reversible process, and that which can be obtained from a real (irreversible) process. Thus,

$$\dot{W}_{act} = \dot{W}_{rev} - T_o \dot{\Pi} \tag{2.18}$$

2.2 Exergy Balances

An exergy balance, written for an open system, has the form

$$\frac{dE}{dt} = \sum_b \dot{E}^{Q_b} - \dot{E}_{pdv} - \dot{W}_x + \sum_i \dot{n}_i \epsilon_i - T_o \dot{\Pi} \tag{2.19}$$

where $\frac{dE}{dt}$ is the rate of accumulation of exergy in the system, $\dot{E}^{Q_b}$ is the rate of exergy input with heat Q at a point b on the system boundary, $\dot{E}_{pdv}$ is the rate of exergy output with work due to volume change, $\dot{W}_x$ is the rate of shaft work output, $\dot{n}_i \epsilon_i$ is the molar flow rate of exergy with matter into the system at point i, and $T_o \dot{\Pi}$ is the rate of exergy destruction over the volume of the system, also known as the irreversibility.

As is shown by the exergy balance, of the total exergy input to a process, some exits in the form of products, some is destroyed due to irreversible processes, and some exits in the form of waste streams such as cooling water of stack gases. Typically a waste stream will have a low exergy value (relative to the exergy input or to the exergy of the main product). If a waste stream has a high exergy value, this represents a high potential to do work, and so the waste stream may be reconsidered as a marketable commodity.

A useful concept is that of energy grade. This indicates the ability of energy to do work.

$$energy\ grade = \frac{exergy}{energy} \tag{2.20}$$

For the case of thermal energy, the ability to do work depends on the temperature of the reservoir from which heat is drawn.

$$energy\ grade = \frac{\dot{Q}(1 - \frac{T_\circ}{T})}{\dot{Q}} = (1 - \frac{T_\circ}{T})$$

Work itself is an ordered energy transfer and has an energy grade of unity. For a chemical reaction, the maximum work is given by the change in Gibbs function for the reaction. Thus,

$$energy\ grade = \frac{(G_R - G_P)}{(H_R - H_P)} = 1 - \frac{T_\circ(S_R - S_P)}{(H_R - H_P)}$$

This value may be greater or less than unity.

2.3 Second Law Efficiencies

The word efficiency, in common usage, indicates the degree to which waste is minimized in the provision of services. For example, people may manage their time efficiently, and thus be able to perform more tasks, or people may talk about the efficiency of the post office in delivering the mail. Efficiency in these contexts is subjective.

In engineering, efficiency is normally quantified. This quantification should indicate the degree to which the performance of a task approaches ideal, that is, produces minimum waste. It is always some ratio of output quantities to input quantities. The efficiency of an electric motor is 100% only if all of the electric power input to the motor manifests itself in the form of rotating shaft power output. This is never the case in a real motor; some electricity is changed into heat, ultimately serving to increase the internal energy of the motor or its surroundings. As a result, the electric motor has an efficiency of less than unity.

This quantification for thermal systems has led to an energy efficiency (η) defined as

$$\eta = \frac{energy\ in\ desired\ products}{total\ energy\ input} \tag{2.21}$$

For a heat engine, this first law (*energy*) efficiency is expressed as

$$\eta = \frac{work\ output}{heat\ input}$$

In the case of an ideal reversible (Carnot) heat engine, this ratio collapses to

$$\frac{T_H - T_C}{T_H}$$

For any value of T_C other than 0°K, this expression is less than unity. Therefore, this quantity does not measure efficiency, as efficiency is understood by the lay person. That is, it is not an indication of the waste produced in the delivery of services. Furthermore, any real device will have a ratio of energy fluxes less than the ideal. Thus, both natural and design constraints are included in such an expression.

Similarly for an ideal heat pump (reversed Carnot engine) or a refrigerator, the ratio of energy flows is, respectively

$$\frac{T_H}{T_H - T_C} \quad or \quad \frac{T_C}{T_H - T_C}$$

This quantity will be greater or less than unity (respectively) for the ideal device. Thus, again a ratio of energy flows does not represent a measure of approach to ideal, when the ideal is defined as 100%. Engineering practice and terminology recognizes this, and in the case of heat pumps and refrigerators, the term Coefficient of Performance (COP) is used to identify these ratios of energy fluxes.

These examples illustrate that the ratio of energy fluxes commonly used as a figure of merit do not represent the degree to which services are provided in a non-wasteful (ideal) manner. Efficiencies expressed in terms of energy can be misleading to the lay person. The essence of science in presenting ideas is clarity and illumination of the subject. In order to discover an expression for efficiency such that the ideal is defined as 100%, the second law of thermodynamics is required. The ideal is defined as a reversible process, and efficiencies are expressed in terms of ratios of second law quantities, specifically, exergy fluxes. For the purposes of this thesis, two types of second law efficiencies are defined as follows:

Effectiveness (ψ) is the ratio of exergy output in products to exergy input to create those products.

$$\psi = \frac{exergy\ output\ in\ products}{exergy\ input} \tag{2.22}$$

Exergy efficiency (η_ξ) is

$$\eta_\xi = \frac{exergy\ output\ as\ service}{exergy\ input\ to\ provide\ that\ service} \tag{2.23}$$

(which is analogous to the energy efficiency (η) defined above).

To illustrate the difference in the two efficiency definitions, consider a pump which moves a fluid such as water from a reference state and level up to a higher level. The water gains some potential exergy because it is at a higher elevation. The effectiveness and the exergy efficiency are the same in this case, because

the service provided is identical to the exergy output and the exergy input is simply electricity (liquid water from the reference environment has no exergy). However, if the fluid pumped is methanol, then the effectiveness becomes much higher than the exergy efficiency. The pumped methanol may have both chemical and potential exergy. The total exergy input is the exergy of the methanol (including chemical exergy) plus the exergy (electricity) required to power the pump. The exergy of the methanol is much larger than the electricity input required, so that effectiveness approaches unity. Effectiveness, then, says nothing about how closely the performance of the pump approaches ideal. The exergy efficiency, however, will be similar to the first case when the fluid pumped was water. It may vary due to different fluid properties, such as compressibility. Exergy efficiency is a measure of pump performance. The service provided is that of pumping methanol from one elevation to another: it is the exergy that the methanol gains due to elevation change. The exergy input to provide that service is simply the electricity to power the pump.

It is not that one expression is correct, and the other incorrect. Rather there is value in the different perspectives. Exergy efficiency (η_ξ) measures the degree to which the ideal is approached in performing a task. A high exergy efficiency indicates low irreversibilities and losses. Exergy efficiency is a measure of process performance or quality. Alternatively, effectiveness (ψ) indicates the amount of exergy input to perform a process relative to the exergy of the commodity being processed. From the perspective of total exergy input to a process, perhaps in terms of resources, effectiveness indicates the degree to which those resources are utilized to perform services. A low effectiveness indicates that a lot of exergy supplemental to that of the commodity being manipulated is required.

2.4 Exergy of Emissions

All emissions have some exergy and thus may disturb the equilibrium of the environment [20, 25, 26]. Considering the processes investigated in this study, emission streams fall into two categories: heat emissions, consisting of waste heat removed typically by water or air cooling, and material emissions, such as combustion products or oxidation products.

The exergy of heat emissions varies due to the magnitude of the heat flow and the temperature at which heat is released into the environment. Heat emissions may be considered the least environmentally disruptive of all emissions [27]. That is to say, a unit of chemical exergy emitted will probably have a greater environmental impact than a unit of thermal exergy emitted. For the most part heat emissions are dissipated in the environment, and thus the potential to do work on the environment is destroyed (that is, their exergy is destroyed). Some heat emissions may do work in the lifting of gases into the upper atmosphere, however this effect is small compared to the circulations caused by solar heating of the earth. Exergy is simply destroyed by creating entropy. This additional entropy may add to the degradation of the environment. Although on a large scale the planet rids itself of entropy with reflected long wave radiation, locally heat emissions resulting in increased entropy can have some effect on the environment. For example, the temperature in a city may be greater than that in the surrounding country. This would likely result in more air conditioning, using more electricity thus creating more heat and consuming more resources. The environmental impact of heat emissions may be faster depletion of resources and increased entropy. In a lake from which cooling water is drawn, the warmer temperature of the water near the outlet may result in increased marine life in that vicinity.

Thermomechanical exergy of material emissions results from the material stream having different temperature and/or pressure than the environment.

It is conceptually easy to obtain work from a system that is at a different pressure than the environment simply by adding a turbine operating between the system and the environment. This could be used to produce electricity or some other useful effect such as compression power. Alternatively, the exergy of a system at high pressure could be destroyed by the use of a throttling valve. Material streams are generally exhausted at or near ambient pressure for the these reasons. Emissions having high temperature behave similarly to the heat emissions discussed above. Thus, the thermomechanical exergy of emissions can not account for much work done on the environment however it may add to the increased entropy (and degradation) of the environment.

Chemical exergy also contributes to environmental impact. Chemical exergy is a function of the composition of both the system and the reference environment. The amount of work that is done on the environment is a function of the processes which bring the material stream into equilibrium in the environment. A substance may undergo many chemical transformations before its elements reach their final stable states in the environment. Exergy is defined as the *maximum* amount of work that a system can perform when it goes into equilibrium with the environment. There are always irreversibilities, so some exergy will be destroyed. Those irreversibilities are proportional to the production of entropy. It follows that if one emission stream has greater chemical exergy than another, then it has greater potential for environmental impact.

The chemical exergy of substances which are part of the reference environment is based on the concentration difference of that substance between the system and the environment. When considering environmental impact, it may be construed that diluting the concentration of a substance in a system will reduce its chemical exergy (although increase the system mass) and thus solve the problem of a high exergy emission. Then, dilution can be perceived as an acceptable method of pollution control. Experience has shown that this is not always the case. Again, some caution is necessary in relating environmental impact to emission exergy.

For energy sources, thermomechanical exergy is most often[3] small compared to chemical exergy. This is noted in Section 5.2 where methane inlet conditions to a compressor are examined. Until methane reaches states having high temperature and/or pressure, its chemical exergy is much greater than its thermomechanical exergy, and so comprises most of its total exergy. Methane, being a part of the natural environment, may be expected to have little or no chemical exergy. However, this expectation is flawed because methane, in large quantities, is constrained by geological formations in the natural environment. It is not in equilibrium with other environmental substances. As well, methane is not part of the reference environment with respect to which exergy is calculated (its concentration in the atmosphere is less than 0.01% by volume). The constrained methane in the natural environment constitutes a system of high exergy, and is considered a resource. Methane emissions from rice paddies, however, represent unconstrained systems of high exergy, and are not resources due to their unconstrained nature. These emissions are broken down into carbon dioxide and water, which are substances found in the reference environment.

The choice of the phrase *environmental impact* instead of *environmental damage* is intentional. Damage is subjective and must be evaluated with respect to some set of values. It has been argued that exergy fails to account for toxicity, however, in evaluating a toxic effect the environment has changed from the standard reference environment used in this study to the environment of the body of an organism. Exergy is a property of a system and its environment, and some judgement is necessary in defining the environment. It is perhaps a limitation of exergy analysis that the biosphere is not included in the reference environment.

[3]fossil sources, not necessarily geothermal, hydraulic, OTEC, etc.

2.5 Modeling Thermodynamic Properties of Substances

All substances with the exception of methanol are modeled as simple compressible substances. Mixtures are either ideal gas mixtures obeying Dalton's law of partial pressures or ideal solutions. The primary source of equations which model the properties of substances is Reynolds [28]. Air is modeled as an ideal gas mixture of nitrogen, oxygen, water vapour, carbon dioxide, and inert gases. Methanol is modeled using the work of Goodwin [29] which compares well with experimental data. The hydrogen molecule exists in two states (ortho hydrogen - the state in which the two electrons spin in the same direction, and para hydrogen - the lower energy state in which the two electrons spin in opposite directions). Roder et al have developed models for equilibrium and para hydrogen [30]. Equilibrium hydrogen is a mixture of ortho and para hydrogen, in their equilibrium proportions corresponding to any given temperature. For example, at room temperature, the stable state of hydrogen is 75% ortho and 25% para. At states below the normal boiling point, hydrogen is virtually 100% in the para state. The equilibrium hydrogen model was used in this analysis whenever it was possible.

Chapter 3

Methanol Pathways

3.1 Methanol Production

Methanol can be produced by steam methane reforming combined with catalytic synthesis. The reforming reaction

$$\begin{array}{rcrcrcrcrl}
CH_4 & + & H_2O_{(g)} & + & Q & \rightarrow & CO & + & 3H_2 & \\
\text{-}74.9 & + & \text{-}241.8 & + & 206.2 & \rightarrow & \text{-}110.5 & + & 0 & \text{MJ/kgmole of } CH_4 \\
802.3 & + & 0 & + & 206.2 & \rightarrow & 283.0 & + & 725.5 & \text{MJ/kgmole of } CH_4
\end{array}$$

produces a mixture of carbon monoxide and hydrogen known as synthesis gas. As well as the reaction, two enthalpy balances are shown. The first balances the standard enthalpies of formation of the various substances involved. The second balances the heats of combustion of each substance. Each energy balance shows that the reforming reaction is strongly endothermic. The second balance is valuable because it readily shows the energy in the products. All chemical reactions shown in this thesis are followed by these two energy balances.

The slightly exothermic shift reaction also occurs.

$$\begin{array}{rcrcrcrcrl}
CO & + & H_2O_{(g)} & \rightarrow & CO_2 & + & H_2 & + & Q & \\
\text{-}110.5 & + & \text{-}241.8 & \rightarrow & \text{-}393.5 & + & 0 & + & 41.2 & \text{MJ/kgmole of CO} \\
283.0 & + & 0 & \rightarrow & 0 & + & 241.8 & + & 41.2 & \text{MJ/kgmole of CO}
\end{array}$$

Finally, the methanol synthesis reactions occur in the presence of a nickel-based catalyst [31].

$$
\begin{array}{rcrcrcrl}
CO & + & 2H_2 & \rightarrow & CH_3OH & + & Q & \\
-110.5 & + & 0 & \rightarrow & -200.9 & + & 90.4 & \text{MJ/kgmole of } CH_3OH \\
283.0 & + & 483.7 & \rightarrow & 676.3 & + & 90.4 & \text{MJ/kgmole of } CH_3OH
\end{array}
$$

$$
\begin{array}{rcrcrcrcrl}
3H_2 & + & CO_2 & \rightarrow & CH_3OH & + & H_2O_{(g)} & + & Q & \\
0 & + & -393.5 & \rightarrow & -200.9 & + & -241.8 & + & 49.2 & \text{MJ/kgmole of } CH_3OH \\
725.5 & + & 0 & \rightarrow & 676.3 & + & 0 & + & 49.2 & \text{MJ/kgmole of } CH_3OH
\end{array}
$$

These reactions are both exothermic.

Rosen [25] has examined the Imperial Chemical Industries methanol production process from both the energy and exergy perspectives. The analysis in this thesis utilizes the material and energy flows as given in [25]. Pure methane is input to the process both as a feedstock and a fuel, and is the only source of both energy and exergy for the process. Air and water are also process inputs, but being part of the reference environment, neither possesses any exergy. A simplified process diagram indicating material and exergy flows is shown in Figure 3.1.

Methanol is the primary product, and leaves the process at a different temperature and pressure than that of the environment. It is assumed that this thermomechanical exergy is destroyed by interaction with the environment and this exergy penalty is applied to the methanol production process. Power in the form of shaft work or electricity is a by-product of this process. It acts as an exergy credit as shaft power is a valuable commodity if it can be used on-site or sold. The effectiveness of methanol production is 0.409. In this case, effectiveness and exergy efficiency have the same value.

Emissions consist of stack gases from combustion and energy in the form of heat. The exergy of emissions accounts for 0.06 units of exergy leaving the process per unit of exergy input. The breakdown is shown in Table 3.1.

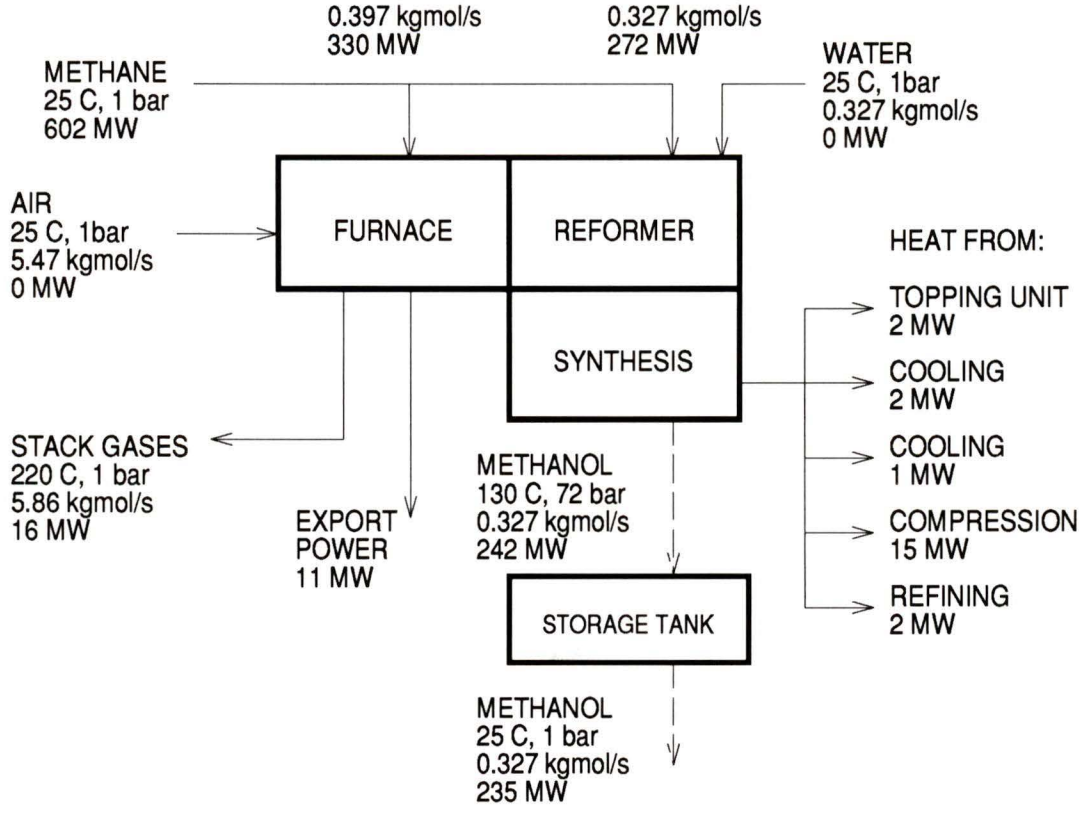

Figure 3.1: Methanol production process: material and exergy flows, based on a 900 ton/day plant.

3.2 Methanol/Fuel Cell Route

3.2.1 On-Board Steam Methanol Reforming

Methanol is attractive as an energy currency for transportation applications because it is a liquid at ambient conditions. The generation of hydrogen from methanol using steam reforming has been previously investigated [32, 33, 34, 35]. These studies have concentrated on automotive applications utilizing exhaust gas heat from the internal combustion engine and/or heat from the engine coolant to provide energy for the reforming reactions. Others [36, 37] have suggested catalytic decomposition by partial oxidation as a means of deriving

Table 3.1: Exergy of Emissions from the Methanol Production Process

Emission	Exergy per Unit Exergy Input
Stack Gas	0.0263
Heat from: Topping Unit	0.0032
First Cooler	0.0033
Second Cooler	0.0009
Compression	0.0253
Refining	0.0026
Total	0.0615

hydrogen from methanol, but again with respect to optimizing internal combustion engine performance, so that carbon monoxide could be considered a desirable product. However, hydrogen is the sole desirable product when a fuel cell is the energy conversion technology. Furthermore, it is advantageous for all of the carbon monoxide to oxidize to carbon dioxide so that separation of the hydrogen fuel from the other reforming products before being input to the fuel cell is not necessary (carbon monoxide will poison the platinum electrodes of the fuel cell, leading to high maintenance costs). The effectiveness of catalytic decomposition will be lower than that of steam reforming, so only steam reforming is considered here.

Methanol must be reformed to hydrogen in order to be useful in a solid polymer fuel cell. The ideal reforming reaction at standard conditions is

$$
\begin{array}{rcrcrcrcrl}
CH_3OH_{(l)} & + & H_2O_{(l)} & + & Q & \rightarrow & CO_2 & + & 3H_2 & \\
\text{-}238.8 & + & \text{-}285.8 & + & 131.1 & \rightarrow & \text{-}393.5 & + & 0 & \text{MJ/kgmole of } CH_3OH \\
638.3 & + & \text{-}43.9 & + & 131.1 & \rightarrow & 0 & + & 725.5 & \text{MJ/kgmole of } CH_3OH
\end{array}
$$

Heat for the vaporization of water and methanol, and for the reforming reaction itself, is supplied by the combustion of methanol (assumed to be complete) with 40% excess air. Realizing that the fuel cell requires pressurized hydrogen, it is prudent to carry out the reforming reaction under pressure (as it requires much

less work to pressurize a liquid than a gas). Reforming is assumed to take place at 4 bar. The products are assumed to take their equilibrium concentrations at 505 K. Material and exergy flows for the process are shown in Figure 3.2.

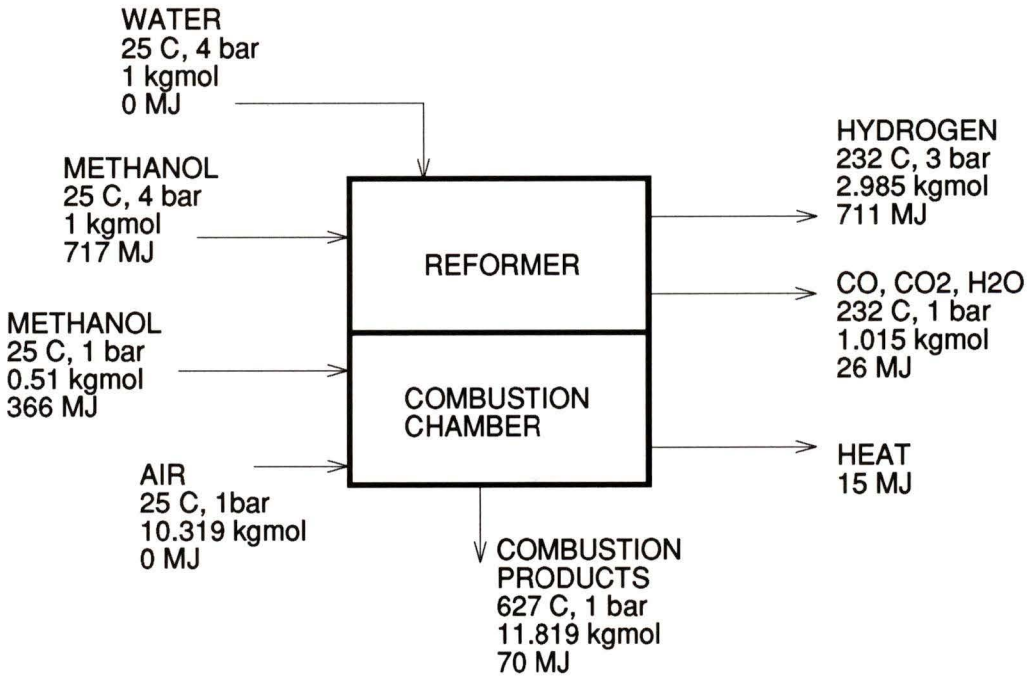

Figure 3.2: On-board reforming of methanol: material and exergy flows.

Hydrogen is assumed to be separated from the product stream using an ideal semi-permeable membrane. A pure hydrogen stream at 3 bar is fed into the fuel cell. The effectiveness of the steam methanol reforming process is 0.657. Again the exergy efficiency of this process is the same as the effectiveness. Emissions from this process consist of waste product gases and low-grade heat. Heat is assumed to be removed via the circulation of a heat transfer fluid, such as water. The exergy of emissions (from Figure 3.2) are:

70 MJ/kgmole of methanol reformed, combustion gases

26 MJ/kgmole of methanol reformed, product waste gas

15 MJ/kgmole of methanol reformed, heat at 75 °C

It is further assumed that either the reformer will be able to produce hydrogen at the rate required by the fuel cell or that some intermediate storage will be available at no exergy cost.

3.2.2 Currency to Service Transformation

Pure hydrogen is fed into the fuel cell. The fuel cell under consideration, developed by Ballard Power Systems, is of the solid polymer variety, utilizing an acid (proton exchange) membrane. This fuel cell operates at 3 bar and 80°C. Air must be compressed to 3 bar, methanol and water are pumped to 4 bar for the reforming process, and cooling water is circulated around both the fuel cell and reformer. The compressor and pumps add a parasitic, load dependent, demand to the fuel cell power output. A stack of 100 cells is able to provide power throughout the required range. Details are shown in Figure 3.3.

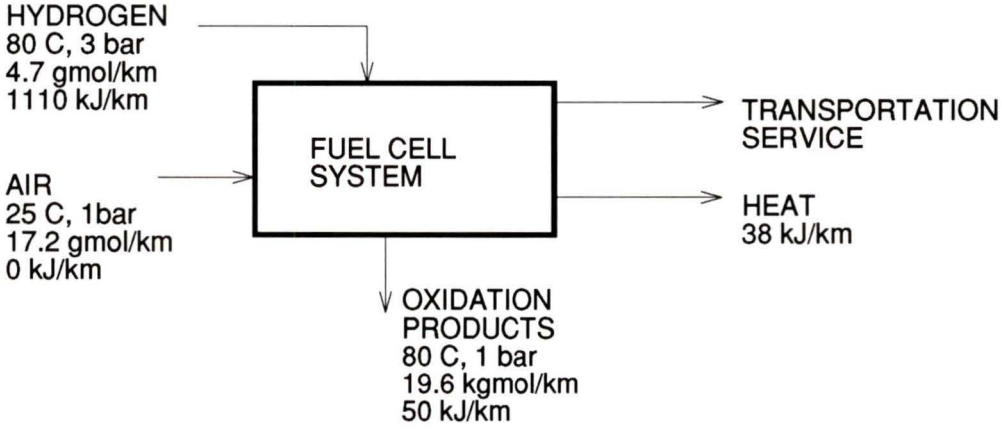

Figure 3.3: Fuel cell operation with steam reformed methanol as the fuel: material and exergy flows.

The energy service is defined as one kilometer of city driving, as described in Appendix B. Fuel cell effectiveness is a straightforward calculation. Exergy output from the fuel cell is the cumulative power produced in each one-second

interval of the duty cycle ($V \times I \times \Delta t$), less the power required to run the air compressor and other auxiliary devices mentioned above. Exergy input is simply the total mass of fuel used over the duty cycle multiplied by the specific fuel exergy. The fuel cell effectiveness over the cycle averages 0.539, with a hydrogen consumption of 9.41 g/km (1110 kJ/km). The total exergy of emissions (including heat) is 88 kJ/km, which is about 8% of the hydrogen exergy input to the fuel cell. The fuel cell exergy efficiency is the same as its effectiveness.

3.3 Methanol/Spark Ignition Engine Route

3.3.1 Currency to Service Transformation

The familiarity of liquid fuels teamed with internal combustion engines perhaps explains in part the acceptance of methanol as a viable alternative fuel. Much research concerning methanol has concentrated on methanol–gasoline blends, typically from 85% to 95% methanol. Here, only 100% methanol fuel is considered. The results presented are based on a U.S. EPA evaluation of a spark-ignition engine optimized for methanol fuel by Toyota. Fuel consumption and emissions data over the FTP[1] dynamometer schedule are taken from [38] and are summarized in Table 3.2.

The results from the three tests were averaged. The control system was optimized for best driveability, which would imply rich mixtures for acceleration and lean mixtures under steady and deceleration conditions. It was assumed that average air fuel ratio would be stoichiometric. Hydrocarbon emissions were taken as entirely methane for the purpose of emission exergy calculation.

It is not possible to calculate exergy output from the engine directly because instantaneous speed torque measurements from the tests are not available. The effectiveness of the engine is found by comparison of exergy input to the engine with exergy input to the fuel cell. This method implies that the exergy required

[1] Federal Test Procedure, see Appendix B

Table 3.2: Fuel Consumption and Emissions from a Methanol Fueled Spark Ignition Engine[2]

Emissions (g/km)	Test 1	Test 2	Test 3
HC[3]	0.018	0.014	0.24
CO	1.191	2.59	0.72
NO_x	1.223	0.79	0.9
HCOH	0.0182	0.014	0.046
CH_3OH	0.409	0.35	0.64
Fuel Consumption (g/km)	104.	97.	88.

[1]Adapted from [38].
[2]HC (hydrocarbons) do not include HCOH (formaldehyde) and CH_3OH (methanol).

to provide the service is the same from each device. The effectiveness of the engine is found to be 0.278. The exergy efficiency of the engine is the same as the effectiveness because the service provided and the total exergy input are identical in each case.

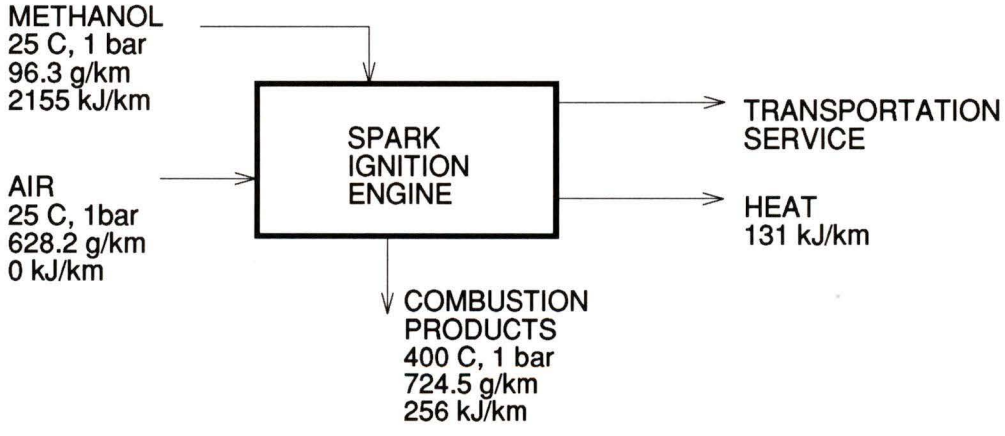

Figure 3.4: Spark ignition engine fueled by methanol: material and exergy flows.

The exergy of material emissions from the methanol engine, shown with other exergy flows in Figure 3.4, was calculated as 256 kJ/km, of which just under half is chemical exergy. Tail pipe exhaust conditions are taken as 400°C,

1 bar, for the calculation of thermomechanical exergy. The temperature of heat emissions from the water cooled engine is taken as 80°C, yielding 131 kJ/kg for a total (heat and mass) emission exergy of 381 kJ/km. Emissions account for over 17% of the fuel exergy input.

Chapter 4

Hydrogen Pathways

4.1 Hydrogen Production

Steam methane reforming (SMR) is the most common method of bulk hydrogen production for consumers other than petroleum refineries [39]. The reforming reaction produces synthesis gas, and is followed by the shift reaction which completes the conversion of methane to carbon dioxide and hydrogen. The reforming reaction is

CH_4	+	$H_2O_{(g)}$	+	Q	$\rightarrow$	CO	+	$3H_2$		
-74.9	+	-241.8	+	206.2	$\rightarrow$	-110.5	+	0		MJ/kgmole of CH_4
802.3	+	0	+	206.2	$\rightarrow$	283.0	+	725.5		MJ/kgmole of CH_4

The shift reaction is also as previously shown

CO	+	$H_2O_{(g)}$	$\rightarrow$	CO_2	+	H_2	+	Q		
-110.5	+	-241.8	$\rightarrow$	-393.5	+	0	+	41.2		MJ/kgmole of CO
283.0	+	0	$\rightarrow$	0	+	241.8	+	41.2		MJ/kgmole of CO

The final steps in the SMR process involve the separation of hydrogen from carbon dioxide.

This thesis utilizes the material and energy flows shown by Rosen [25] for the SMR process. The resulting exergy flows are illustrated in Figure 4.1.

Exergy enters the process solely with methane, which is both feedstock and fuel. The process waste streams consist of stack gases and cooling water. As

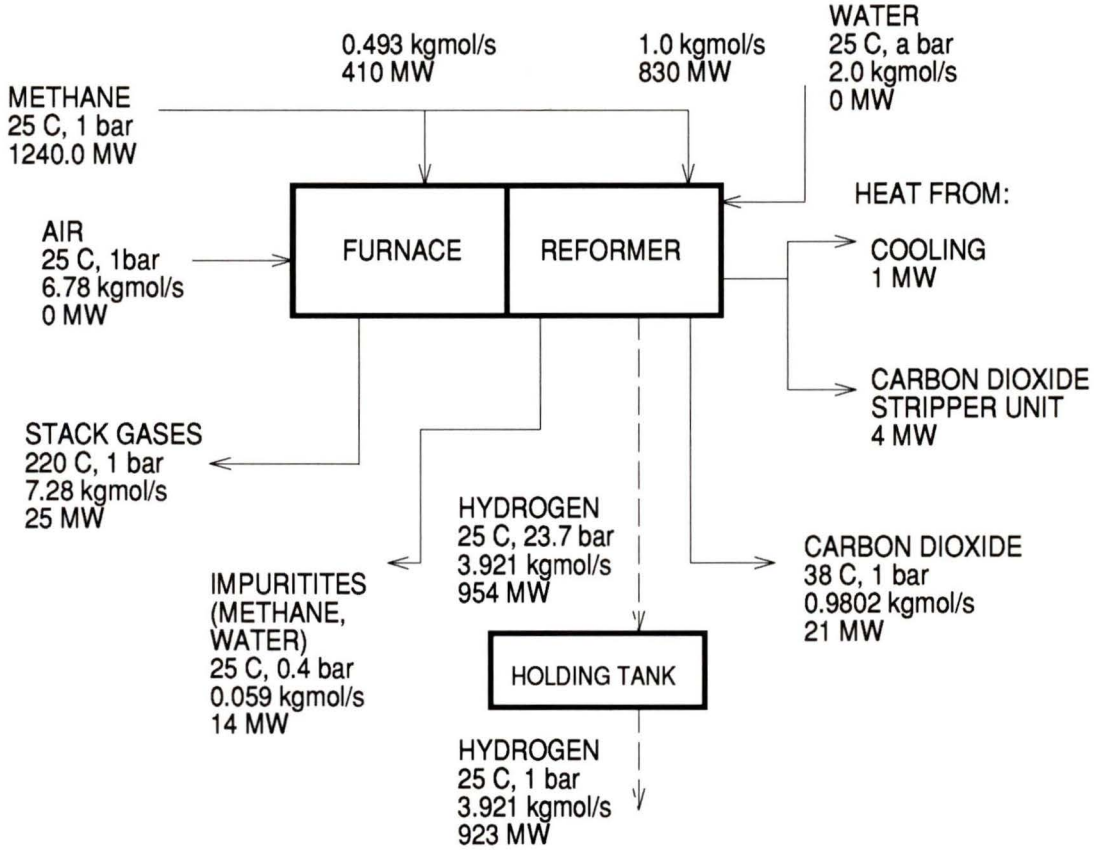

Figure 4.1: Steam methane reforming for the production of hydrogen: material and exergy flows based on a 700 ton/day plant.

for the case of methanol production, the product hydrogen actually leaves the process at elevated temperatures and pressures (with respect to environmental conditions). Both the work of hydrogen compression and the work of liquefaction are based on hydrogen entering at ambient conditions, so 25°C, 1 bar is taken as the exit state of hydrogen from the production plant. The change in pressure of the hydrogen may be used to produce export power, however this is not assumed in this scenario. Consequently, the effectiveness of hydrogen production is 0.744.

Methane combustion, which provides process heat and electricity, results in stack gas emissions. As well, carbon dioxide and trace amounts of methane

and water are rejected. The total exergy of emissions (including both heat and material emissions) is about 5% of the exergy input to the process.

4.2 Liquid Hydrogen/Fuel Cell Route

4.2.1 Liquefaction of Hydrogen

Hydrogen is attractive as a fuel because it has the highest energy density per unit mass of all chemical fuels. The primary disadvantage of liquid hydrogen fuel is that special cryogenic devices are required for its storage and handling. These devices add weight and bulk to any vehicle. At atmospheric pressure, pure hydrogen liquefies at a temperature of 20 K. A considerable amount of work (in the thermodynamic sense) is required to produce liquid hydrogen at these conditions. Although new technologies, such as magnetocaloric methods, are under development [40, 41, 42] and promise great reductions in this work requirement, conventional liquefaction technology is considered in this thesis.

The conventional process considered begins with the precooling of hydrogen against some refrigerant. Then, the gaseous hydrogen is compressed to a working pressure near 600 psi. It is cooled against recycle hydrogen streams, and also against nitrogen. A liquid nitrogen bath surrounding a catalyst is used to accelerate the ortho- to para- conversion. The hydrogen is further cooled against recycle streams of hydrogen, which themselves undergo expansion cooling through turbines. Finally, the hydrogen is throttled to just over 1 bar, undergoing Joule-Thompson cooling. The recycle hydrogen streams are compressed, and rejoin the incoming feed hydrogen. This analysis relies on papers by Dini [43] and by Baker and Shaner [44] which both assume theoretical plants with a capacity of 250 ton/day. Figure 4.2 shows the liquefaction process as a *black box*, with a work requirement estimated from those given in [44, 43].

Currently there are no liquid hydrogen production plants operating with such a large capacity (250 tons/day). Strobridge [45] has shown that the exergy

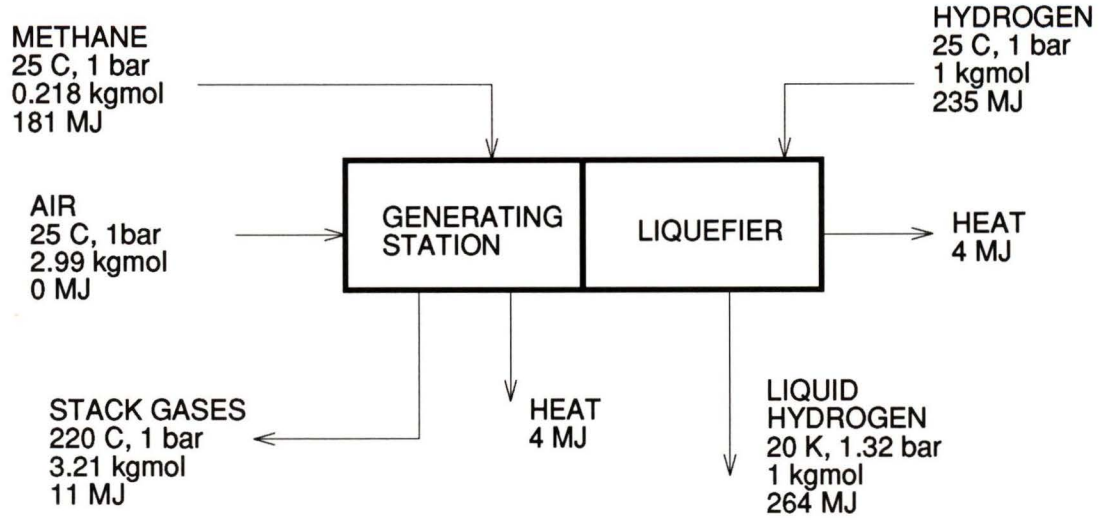

Figure 4.2: Hydrogen liquefaction exergy flows based on a 250 ton/day plant using conventional compression/expansion/heat exchange techniques.

efficiency of conventional hydrogen liquefaction plants increases with increasing capacity, up to a limiting point of about 38%. The exergy efficiency of the hydrogen liquefaction plant shown here is 36%. Currently there are no hydrogen liquefaction plants operating near this efficiency. In fact, the maximum exergy efficiency of hydrogen liquefaction is about 25%, and this may be achieved by plants operating between the 5 ton/day and 66 ton/day capacities. However, the 250 ton/day theoretical plant is used here so as to be reasonably comparable to the 3000 ton/day[1] methane liquefaction plant analyzed later (Section 5.1.1). As a result, this plant represents a *best case* scenario, so that conventional technology cannot be expected to make any improvements in effectiveness (calculated to be 0.635) or exergy efficiency.

Most emissions originate from the combustion of methane to produce electricity. The power generation plant is assumed to have a thermal efficiency of

[1]Note that the 3000 ton/day plant is actually three liquefaction lines of 1000 ton/day operating in parallel, so that the plant exergy efficiency is the same as that for a 1000 ton/day plant.

45% [46], based on efficient combined cycle technologies and the lower heating value of methane. Methane combustion occurs in 40% excess air. Stack gases at 220°C, 1 bar contribute 10.8 MJ/kgmole of hydrogen liquefied to the emission exergy. Cooling water is assumed to be at 38°C, leading to a heat emission exergy of 4 MJ/kgmole of hydrogen liquefied. Similarly, heat rejected from the hydrogen liquefaction process is removed by cooling water, also taken to be at 38°C. This contributes 3.7 MJ/kgmole of hydrogen liquefied to the emission exergy. The total exergy of emissions from this process is 19 MJ/kgmole of hydrogen liquefied, or about 4.5% of the exergy input to the process.

4.2.2 Currency to Service Transformation

The fuel cell simulated is of the solid polymer variety created by Ballard Power Systems. A 100 cell stack with the performance characteristic described in [47] and an electrode area of 0.25 m^3 per plate [48] is sufficient for the average passenger car power requirement throughout the determined duty cycle (described in Appendix B).

Liquid hydrogen is stored on board at about 1.32 bar [49]. This cryogenic fluid is pumped to the fuel cell operating pressure of 3 bar. Heat transfer with the cooling water is used to vaporize the liquid hydrogen. A small compressor, with an isentropic efficiency of 70% is used to compress the incoming air to 3 bar.

Fuel cell effectiveness and exergy efficiency are both calculated as the useful work out divided by the fuel exergy input. The useful work out is that amount of work produced which may go to providing the transportation service. The total work out is the product of voltage and current summed over each one second interval of the duty cycle. The power requirements of the air compressor and circulation pumps on a second–by–second basis were subtracted from the total work output. The resulting value is the amount of work available to provide the transportation service. The exergy input to the fuel cell system is the

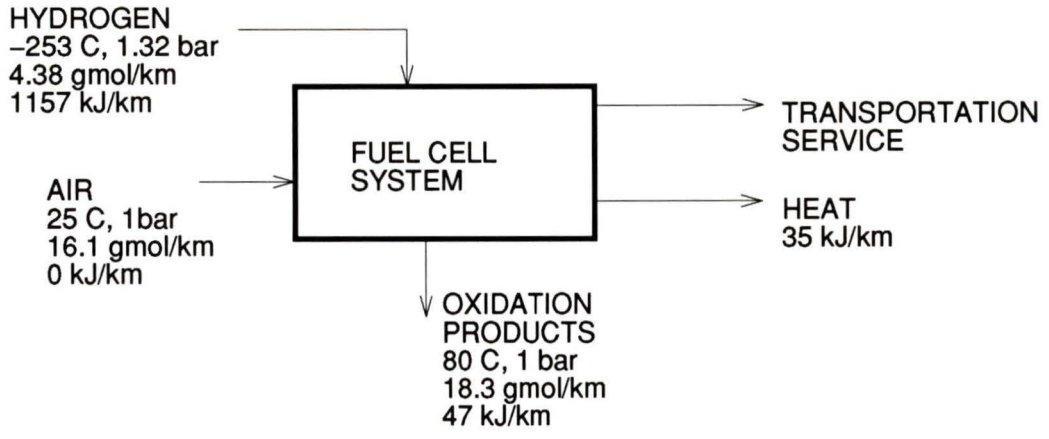

Figure 4.3: Fuel cell operation with liquid hydrogen as the fuel, material and exergy flows.

mass of fuel consumed over the driving cycle, multiplied by the fuel exergy (of liquid hydrogen), divided by the distance traveled. This yields a *per kilometer* normalization. Effectiveness and exergy efficiency of this fuel cell system are 0.521.

Emissions from the fuel cell consist of water vapor and components of air not involved in the cell reaction. The fuel cell operates with 50% excess air. Details are shown in Figure 4.3. Material emissions leave the system at 80°C and 1 bar. The chemical exergy of emissions is 19.0 kJ/km, and the thermomechanical emission exergy is 28.2 kJ/km. Heat is rejected from the system at 60°C, for an emission exergy of 35.1 kJ/km. The total exergy of emissions amounts to about 7% of the exergy input directly to the fuel cell. Fuel consumption is 8.8 g/km, leading to a total water production of 78.8 g/km.

4.3 Compressed Hydrogen/Fuel Cell Route

4.3.1 Compression of Hydrogen

From the reforming plant, hydrogen is likely to be transported via pipeline to central fueling depots. Hydrogen in the pipeline is taken to be at 25°C, 8 bar. In order to obtain this pipeline state, a single stage isentropic compression (with 75% efficiency) from the production facility output condition was assumed and the work of this compression was added to that calculated based on the following assumptions. The gaseous hydrogen fueling station works by compressing hydrogen to some pressure (351 bar) greater than that required in the vehicle tank (311 bar) so that the high pressure hydrogen can simply be throttled into the vehicle tank. The hydrogen compression process is isentropic, with an isentropic efficiency of 75%. The entire process is schematically shown in Figure 4.4. The practice of compressing gas to high pressures and then throttling it into the vehicle tank is a variation of the method used at local natural gas service stations in Italy [50].

Most emission exergy is produced by the generation of electricity from methane. Again, complete combustion with 40% excess air has been assumed. Stack gases are exhausted at 220°C, 1 bar and the temperature of cooling water output is taken to be 38°C. Total emission exergy is about 1% of the exergy input to the compression process. The effectiveness of this process is 0.812. Such a high value is initially surprising however it is accepted when the high chemical exergy of hydrogen is compared to the amount of work required to perform the compression. The exergy efficiency of this process is 0.210, which would seem surprisingly low. However, the processes of cooling after compression and then throttling into the vehicle tank increase the irreversibilities in this energy transformation.

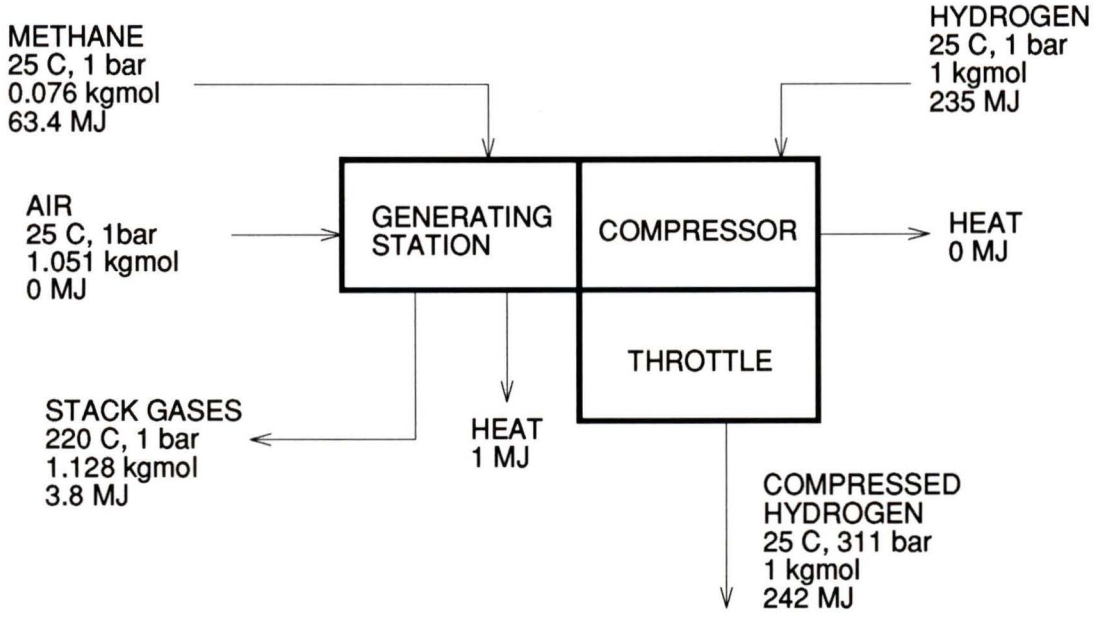

Figure 4.4: Compression of hydrogen: material and exergy flows.

4.3.2 Currency to Service Transformation

Compressed hydrogen is throttled from the vehicle tank storage pressure of 311 bar to the fuel cell operating pressure of 3 bar. Auxiliary devices consist of an air compressor and cooling water pump. Again a fuel cell stack of 100 cells provides power for vehicle operation over the duty cycle. Exergy and material flows are shown in Figure 4.5.

The fuel cell effectiveness over the duty cycle is 0.545, meaning that 0.545 units of transportation service are performed for every unit of exergy input to the fuel cell. Again this figure is identical to the exergy efficiency. Total exergy of emissions amounts to 83 kJ/km, of which about 23% is chemical exergy. The total amount of water produced is 79.4 g/km, which will be shown to be lower than that produced when a spark ignition engine performs the same service.

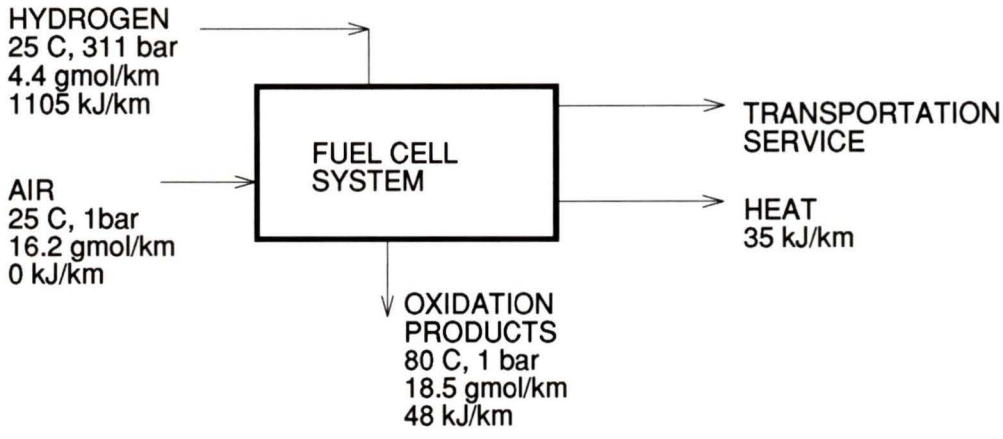

Figure 4.5: Operation of fuel cell using compressed hydrogen fuel: material and exergy flows.

Chapter 5

Methane Pathways

5.1 Liquid Methane/Spark Ignition Engine Route

5.1.1 Liquefaction of Methane

Conventionally, liquefaction of natural gas has been performed on a large scale near the natural gas resource extraction site for the purpose of loading this fuel onto marine tankers for intercontinental shipment. Liquefied natural gas is virtually 100% methane. Several different liquefaction cycles were developed and implemented in the 1960s and 1970s. These include the standard cascade cycle, where three refrigerants are used in independent closed loops to effect cooling; the mixed refrigerant cascade process, where a single multicomponent working fluid is circulated; and a combination process which uses propane as the first refrigerant and then a mixed refrigerant for subsequent cooling. More recently, development work has focussed on Stirling cycle natural gas liquefiers [51, 52]. These can be designed for a wide range of capacities, and operate with an exergy efficiency of about 40%. Information for these Stirling cryocoolers applied to natural gas liquefaction is unavailable beyond the prototype stage. The cascade process, which also has an exergy efficiency of about 40%, is the process which is analyzed in this work. The efficiency of the cascade cycle is greater than either of the processes involving mixed refrigerants [53]. Specifically, the plant at

Arzew, Algeria which liquefies about 3000 ton/day in three parallel liquefaction lines is investigated. Its operation is outlined in reference [54] and is shown schematically in Figure 5.1.

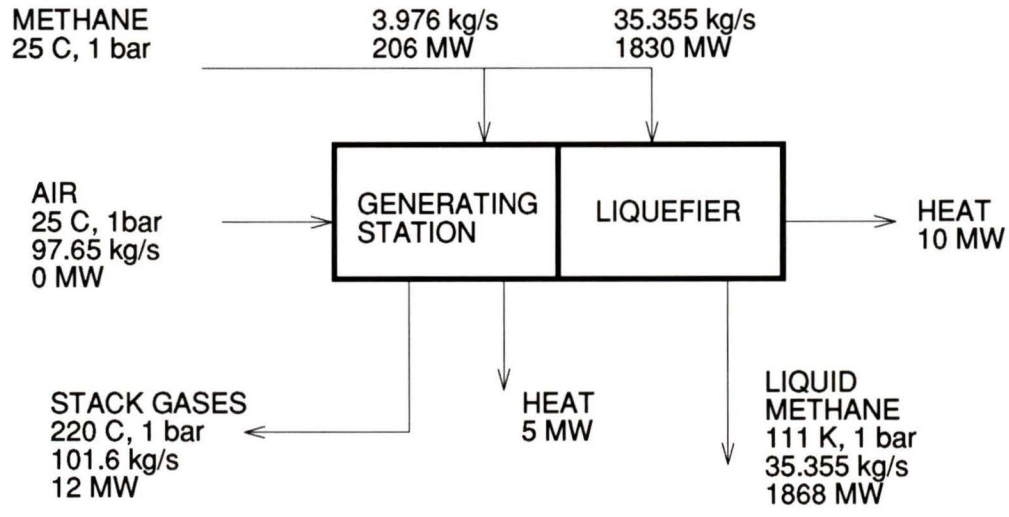

Figure 5.1: Material and exergy flows required for and produced by methane liquefaction using the cascade cycle, based on a 3000 ton/day operation.

Standard inlet conditions are assumed for this process. All power requirements are met either through a methane-fired boiler steam cycle or through a gas turbine engine. The power generation plant was assumed to have an energy efficiency of 45%, based on the lower heating value of methane. The net effectiveness of methane liquefaction is 0.918. This high figure arises due to the small amount of work required to perform liquefaction compared to the large chemical exergy of methane liquefied. The exergy efficiency of this process is 0.41, a much lower number than effectiveness. This, along with the low exergy of emissions, indicates that the liquefaction process involves many irreversibilities. Emission exergy is just over 1% of total exergy input, and is comprised mainly of material emissions. To liquefy methane, heat is removed by the various refrigerants, which in turn give up their heat to cooling water. The temperature at which this water exits the system is 38°C, so this is the temperature at which heat is

released into the environment. This leads to a low exergy of heat emissions.

5.1.2 Currency to Service Transformation

Emission and performance data for vehicles fueled with liquid methane was unavailable. It is expected that engine operation with liquid methane could be substantially different than that with compressed methane as the fuel [55]. Liquid methane, injected directly into the intake or cylinder, cools the incoming air, causing it to contract. This has the effect of increasing the charge density (which is the energy density of the the air/fuel mixture on a volume basis), increasing the volumetric efficiency (which is the ratio of volume of air input to volume displaced by the piston) and decreasing the tendency to preignite (which is ignition without the aid of a spark, occurring spontaneously at high temperature and pressure) [56]. Engine power increases with increasing charge density and increasing volumetric efficiency. Engine power is strongly related to compression ratio. With a cooler intake, the air/fuel mixture may be compressed to higher pressures before auto-ignition occurs. At higher compression ratios, engine performance improves. For the purpose of this analysis it was assumed that liquid methane would be vaporized and warmed through heat exchange with engine coolant prior to entering the intake manifold, so that the emissions and performance of a liquid methane fueled engine would not differ significantly from those of a compressed methane fueled engine.

Emission and fuel consumption data for the methane fueled engine is shown in Table 5.1. The results from the two tests were averaged. It was assumed that average air/fuel ratio would be stoichiometric. Hydrocarbon emissions were assumed to consist entirely of unburnt fuel (methane), for the purpose of emission exergy calculation.

As with the methanol fueled engine, the effectiveness of this engine was found by comparison of fuel exergy input to it with fuel exergy input to the hydrogen fueled fuel cell. With the known effectiveness of the fuel cell, the effectiveness of

Table 5.1: Fuel Consumption and Emissions from Methane Fueled Engine[1]

Emissions (g/km)	Test 1	Test 2
HC	0.80	0.76
CO	0.75	0.06
NO_x	0.75	0.81
Fuel Consumption (g/km)	77.7	74.1

[1]From [57]. Note that the actual engine tests were performed using natural gas fuel. Because natural gas is chiefly comprised of methane, this thesis treats the two as equivalent. The UDDS dynamometer schedule (see Appendix B) was used.

the engine could be calculated and was found to be 0.150. The exergy efficiency is the same, as the service output and fuel exergy input are identical to the total exergy output and input respectively. Note that the exergy of the fuel input is that value at -162°C, 1 bar. The material and exergy flows in and out of the engine are shown in Figure 5.2.

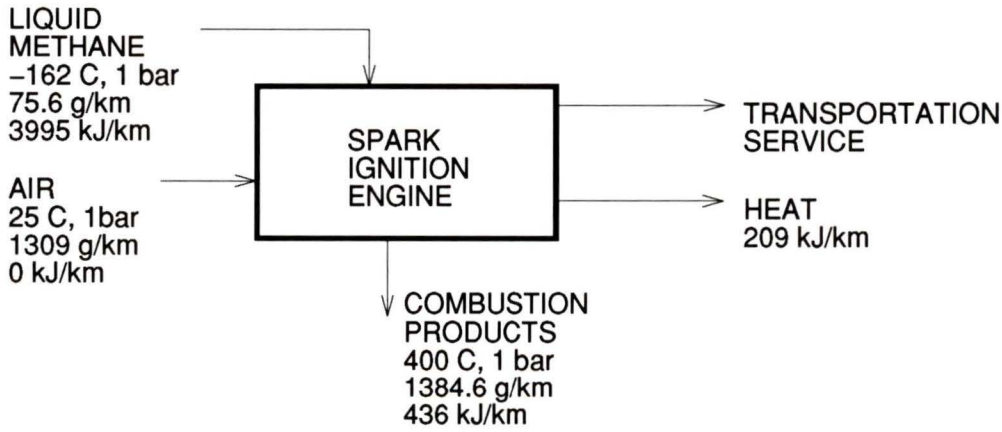

Figure 5.2: Spark ignition engine fueled by liquid methane: material and exergy flows.

Tail pipe exhaust conditions were 400°C, 1 bar. The total exergy of material emissions was found to be 436 kJ/km. Cooling water was taken to be at 60°C so that heat emission exergy amounted to 209 kJ/km. The high emission

exergy and the low engine effectiveness indicate that further optimization of the currency to service transformation should be possible.

5.2 Compressed Methane/Spark Ignition Engine Route

5.2.1 Compression of Methane

Standard inlet conditions of 25°C, 1 bar have been assumed for this pathway, primarily to be consistent with the conditions which methane enters all of the other pathways. In reality, there would probably be a methane pipeline distribution system, from which compressors would draw the fuel. The typical state of natural gas in an underground pipeline in a city is 5°C, 8 bar [58]. The difference in methane exergy at this state is very small compared to the total exergy of methane, because the thermomechanical component is small compared to the chemical component of exergy. This is illustrated in Table 5.2. Although the difference in exergy is small, the variance in pressure has an impact on the energy required for compression if the compression is modeled as isentropic. For this reason, compression was assumed to occur in two intervals. First the gas was compressed isentropically in a single-stage, to 8 bar. After the gas had come to equilibrium, it was then compressed again. This crudely simulates the compression of gas to pipeline pressure followed by compression at a refueling depot. Pipeline losses are neglected because these are distance dependent, and in order to compensate for such losses more compression would be required.

The scenario assumes a local refueling depot exists, which compresses methane from its pipeline state into large holding tanks at 351 bar. The compressor is taken to have 3 stages and an isentropic efficiency of 75%. The methane fuel is then throttled to the nominal pressure of the fuel tank on board the vehicle, which is taken as 311 bar (4500 psi). This is a reasonable pressure for compressed gas tanks aboard vehicles [55]. (This scenario is identical to that

Table 5.2: Exergy of Methane at Various Possible States to be Input to the Compression Process.

State	Exergy (MJ/kgmole)	Difference From Reference State (%)
25°C, 1 bar	830.312	0
25°C, 8 bar	835.437	0.617
5°C, 8 bar	835.462	0.620

developed for the case of compressed hydrogen fuel.)

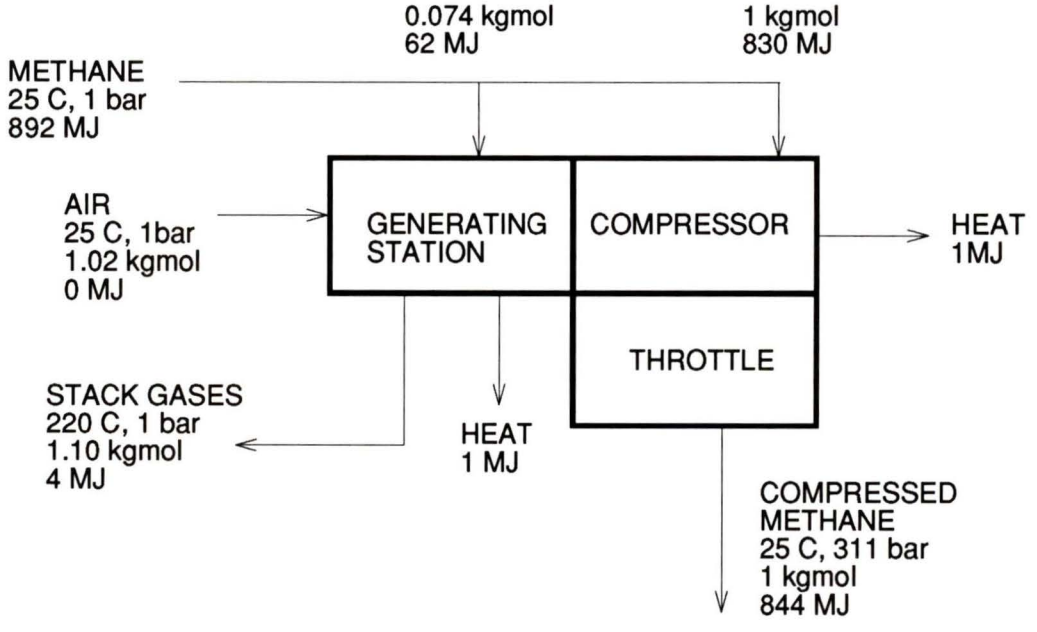

Figure 5.3: Material and exergy flows associated with the compression of methane for use as a transportation fuel.

Figure 5.3 shows the material and exergy flows associated with the methane compression process. Again, electricity production is assumed to have an efficiency of 45% based on the lower heating value of methane. The overall effectiveness of compression is 0.946. This high value is due to the large exergy of methane compared to the amount of work that must be done to provide compression. Another way of looking at this is to consider the exergy input to

make electricity as a function of the exergy of the gas compressed. Just over 7% of the exergy of the compressed gas is required to perform that compression. The exergy efficiency of this process is 0.217, which seems low. However, this number takes into account compression, throttling into the vehicle tank, and electricity generation.

Emissions from the process consist of stack gases from the generation of electricity. As well, heat is emitted. Cooling water is taken to leave the system at 38°. The total emission exergy amounts to less than 1% of the total exergy input.

5.2.2 Currency to Service Transformation

Compressed methane is throttled from the tank storage pressure to about ambient pressure before admission to the intake manifold. Pressure regulating devices have been developed for this purpose [59]. The engine was a retro-fit of an existing gasoline engine, rather than a newly designed, highly optimized methane engine. Emissions have already been shown in Table 5.1. The material and exergy flows associated with the engine are shown in Figure 5.4.

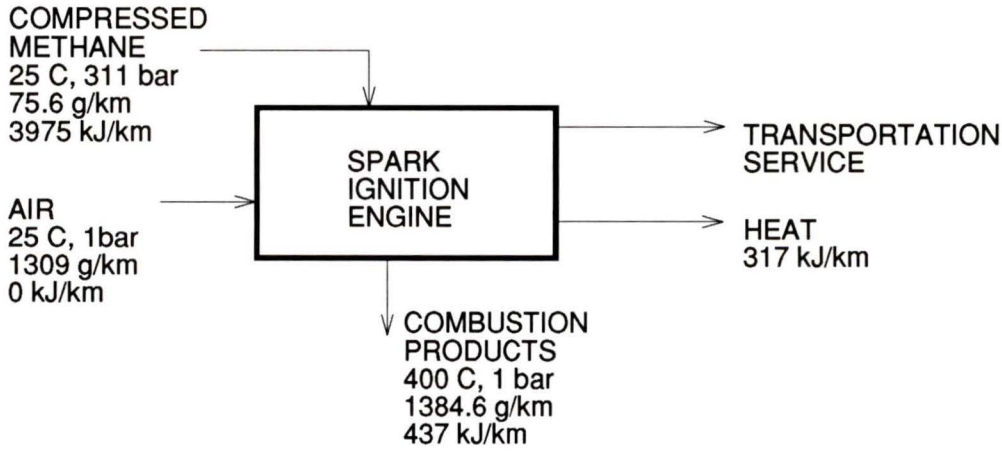

Figure 5.4: Compressed methane fueled spark ignition engine: material and exergy flows.

The effectiveness of the engine is found by comparison of exergy input to the engine with that input to the fuel cell. Knowing fuel cell effectiveness in delivering the identical service, engine effectiveness is calculated. It is found to be 0.151, slightly greater than that for the liquid methane fuel pathway. This is due to the lower exergy of the compressed fuel than the liquid fuel, as the same mass of fuel was used to provide the same service in each case. The emission exergy from the engine totals 754 kJ/km, of which just over half is attributed to the combustion gases.

Chapter 6

Comparison of Pathways for Methane Use in Transportation

Methane, the energy (and exergy) source, is taken to be input to the various routes (as shown in Figure 1.1) at the standard state of 25°C and 1 bar. Methane can be a feedstock for the production of many energy currencies of which three have been examined here: methanol, hydrogen, and methane itself. These currencies were chosen as being likely transportation fuels in the future [60, 55].

The transportation energy service was defined using a city driving schedule[1]. For the routes involving a spark-ignition engine, the effectiveness was calculated based on average fuel consumption over the duty cycle. Explicitly, this gives the exergy input to the vehicular conversion technology required to provide the transportation service. The transportation service then is not defined in energy units explicitly, rather it is defined in *service units*: one kilometer of city driving.

The power requirements of an *average* passenger car[2] undergoing this driv-

[1]Both the 1975 Federal Test Procedure (FTP) and the Urban Driving Dynamometer Schedule (UDDS, which is identically the first 1372 seconds of the FTP) were used. These procedures are widely used for the purpose of engine exhaust emission and fuel economy measurements for passenger cars. The FTP covers 17.88 km in 31 minutes, 16 seconds, and the UDDS covers 12.1 km in 22 minutes, 52 seconds. The FTP and UDDS results were averaged so that the simulated fuel cell vehicle performance would be comparable to internal combustion engine vehicle performance. The methanol-fueled engine tests were performed using the FTP however the methane-fueled engine tests were performed using the UDDS. These duty cycles are further described in Appendix B.

[2]The coefficients in the power-velocity equation (see Appendix B) were calculated from

ing schedule were found and fed into a fuel cell simulation to determine the performance of a 100 cell fuel cell stack. The fuel cell simulation was based on the performance characteristic of the solid polymer hydrogen/air fuel cell developed by Ballard Power Systems. The fuel cell operates with 50% excess air, at a temperature of 80°C and a pressure of about 3 bar absolute [48, 47]. The simulation assumes an isentropic compressor efficiency of 70%, power control at 96% efficiency, and a constant motor efficiency of 90% [61]. The motor efficiency of course will be lower at low loads. Often at low loads in the duty cycle, the vehicle is decelerating or at rest, so the motor is not required to provide torque to the wheels. The expected reduction in motor efficiency is compensated for by greater fuel cell output in such conditions. The fuel cell simulation program listing and output are contained in Appendix C.

6.1 Effectiveness

Figure 6.1 shows the effectiveness of each stage in the source to service pathway, for each pathway. Recall that effectiveness is defined as the ratio of exergy output in products to exergy input to create those products. Another expression of performance is given by the inverse of effectiveness. This represents the total exergy which must be supplied to yield a unit service output. It is shown in terms of total exergy input to each process in the source to service pathway, in Figure 6.2. Methane enters each pathway from two directions: first as the chemical feedstock from which energy currencies are derived and second as the fuel which provides process heat and electricity. The efficiency of generating electricity from methane (for example, associated with the liquefaction and compression processes) was assumed to be 45% [46], based on efficient combined

coastdown test results published in Car and Driver Magazine for four selected vehicles, assumed to be similar to those vehicles tested using the FTP and UDDS. Road power is based on weight and coefficients of drag and rolling resistance. As a result, fuel, fuel storage and power train are transparent to power required as long as average weight, frontal area, and tire characteristics are maintained. The mass (including payload) and frontal area were found to be 1316 kg and 1.769 m^3 respectively, for an *average* passenger car.

cycle technologies and the lower heating value of methane.

	METHANOL		HYDROGEN		METHANE	
			LIQUID	COMPRESSED	LIQUID	COMPRESSED
PATH	FUEL CELL	S. I. ENGINE	FUEL CELL	FUEL CELL	S. I. ENGINE	S. I. ENGINE
SOURCE TO CURRENCY	.409	.409	.744	.744		
LIQUEFY/ COMPRESS			.635	.812	.918	.946
ON-BOARD FUEL CONDITION	.657					
VEHICLE ENERGY CONVERSION	.539	.278	.521	.545	.150	.151
NET PATH EFFEC- TIVENESS	.145	.114	.277	.351	.138	.143

Figure 6.1: Effectiveness of processes in the source to transportation service pathway, with methane as the sole exergy source.

The net path effectiveness is not simply the product of the effectiveness of each process in that path. Rather the net path effectiveness is a weighted product of the effectiveness of each process. Similarly, the total path exergy input to the pathway is neither the sum of the exergy input to each process nor necessarily the total exergy input to the first process.

To illustrate, consider the compressed hydrogen, fuel cell pathway. 1440 kJ of exergy in the form of methane are input to the steam methane reforming (SMR) process. With an effectiveness of 0.744, this indicates that 1070 kJ of exergy in the form of hydrogen are output. These 1070 kJ are input to the compression process, along with an additional 290 kJ of exergy in the form of methane. Together, the total exergy input is 1360 kJ. The product consists of 1105 kJ of compressed hydrogen, which is then input to the vehicular fuel cell

PATH	METHANOL		HYDROGEN		METHANE	
			LIQUID	COMPRESSED	LIQUID	COMPRESSED
	FUEL CELL	S.I. ENGINE	FUEL CELL	FUEL CELL	S. I. ENGINE	S. I. ENGINE
SOURCE TO CURRENCY	4130	5270	1385	1440		
LIQUEFY/ COMPRESS			1820	1360	4350	4200
ON-BOARD FUEL CONDITION	1690					
VEHICLE ENERGY CONVERSION	1110	2155	1155	1105	3995	3975
TOTAL PATH EXERGY INPUT	4130	5270	2175	1730	4350	4200

Figure 6.2: Cumulative exergy (from the energy source methane) required to provide one unit of transportation service (kJ/km city driving).

system and is used to provide the transportation service (which is a kilometer of city driving). The total exergy input consists of 1440 kJ in the form of methane which is used to make the energy currency hydrogen plus an additional 290 kJ in the form of methane which is used to make electricity for the compression process. The total is 1730 kJ of exergy input to the path. Now, the original 1440 kJ used to make hydrogen passes through each process, so that the exergy output at the service level is this exergy input times the product of each process effectiveness. 290 kJ were input at the compression state, so the exergy output at the service level from this contribution is that exergy times the compression process effectiveness times the fuel cell effectiveness. Net path effectiveness becomes:

$$\frac{1440(0.744\times0.812\times0.545)+290(0.812\times0.545)}{1440+290} = 0.351$$

The net path effectiveness is a weighted product of each process effectiveness where the weighting factor is the exergy input to that process.

Attention is drawn to the vehicle energy conversion line of Figure 6.1 because it contains several interesting and initially surprising numbers. First, the effectiveness of the fuel cell is very high in all cases, converting every unit of exergy input into over 0.52 units of electricity for the purpose of motive power on average through the duty cycle. This is related to the fact that the fuel cell is most effective at low loads, and the city driving schedule, being stop–and–go, is comprised mostly of low power requirements. That fuel cell effectiveness decreases with increasing power output can be understood in terms of its voltage/current characteristic. The greatest voltage occurs near open circuit conditions, and is associated with low current and consequently low power output. Voltage decreases as current increases, due to polarization and resistance losses. The net result is increased power, but lower efficiency. External to the fuel cell are auxiliary devices (such as an air compressor and water pump). These devices add a parasitic load which increases with increasing service load (that is, the greater the shaft power demand, the more fuel required, thus the more air compressed and greater cooling required). Fuel cell effectiveness decreases with increasing power output due to increased parasitic load and greater losses.

Fuel cell effectiveness varies, depending on the context in which the fuel cell operates. In the liquid hydrogen fuel cell system, a cryogenic pump increases the pressure of hydrogen to 3 bar (absolute), and then the hydrogen is vaporized. Heat for vaporization may come from the warm water used to cool the fuel cell itself. Liquid hydrogen, the *exergy input*, has some thermomechanical exergy which can be used to provide cooling. Looking at the vehicle energy conversion line of Figure 6.1, the liquid hydrogen fuel cell system shows the lowest effectiveness of the fuel cell systems investigated. This is related to the higher exergy of liquid hydrogen than compressed hydrogen, which is not fully utilized by the fuel cell.

The compressed hydrogen fuel cell system on-board the vehicle has an intermediate effectiveness. Much of the thermomechanical exergy of the compressed hydrogen is destroyed by throttling the fuel to 3 bar. However, the thermomechanical exergy of compressed hydrogen is lower than that of liquid hydrogen, so that the exergy input per unit mass is consequently lower and the effectiveness can be higher. The fuel cell is designed to take advantage of chemical, rather than thermomechanical, exergy.

Still on the vehicle energy conversion line of Figure 6.1, it is seen that the fuel cell supplied with hydrogen from reformed methanol exhibits the greatest effectiveness. Hydrogen is delivered from reforming at precisely the conditions required by the fuel cell. Some work is required from the fuel cell in pumping the methanol and water to 4 bar, the pressure at which reforming occurs. The mass of hydrogen required by the different fuel cell systems is not substantially different: 8.82 g/km for the liquid hydrogen system, 8.88 g/km for the compressed hydrogen system, and 9.41 g/km for the reformed methanol system; however the exergy carried with the hydrogen decreases in each case, with constant service. Thus the effectiveness of each system increases correspondingly.

The heat required for methanol reforming is supplied by combustion of methanol in just under a 2:1 ratio (2 units of methanol reformed per unit of methanol combusted). The vaporization of methanol and water, and the reforming process itself, are modeled to occur at 4 bar. Equilibrium concentrations of the products (H_2, H_2O, CO, and CO_2), at 505 K are calculated. Separation of hydrogen is assumed to take place through an ideal semi-permeable membrane. The combined effectiveness of the methanol reformer fuel cell system exceeds that of the internal combustion engine systems (0.354 compared with 0.278).

The spark ignition engine exhibits effectiveness ranging from 0.15 to 0.28. These values are lower than those for the fuel cell systems. The engine converts chemical exergy to heat, and then converts heat to work. In doing so high temperature exhaust gases are released and heat is rejected into the cooling

system. The two energy conversion steps are inherently not as effective in converting fuel exergy to work as the single step (chemical exergy to work) operation of the fuel cell.

The effectiveness of the methane engine[3] is shown as substantially lower than that of the methanol engine. This should be interpreted with caution. The methanol engine figures are based on a highly optimized engine [38] whereas the natural gas engine figures are based on a retrofit engine [57]. More recent reports concerning dedicated methane spark ignition engines for light duty vehicles [13, 62, 63] have concentrated on steady state operation at different loads, rather than the integrated performance over a driving cycle.

The effectiveness of the engine operating with compressed methane is not significantly different than that of the engine operating with liquid methane. Due to a lack of data concerning dedicated spark ignition engines optimized for natural gas or methane in either liquid or compressed form for light duty vehicles, some assumptions are necessary. It is assumed that the liquid would be vaporized outside the engine, using heat exchange with the engine coolant. Thus, the combustion process and products do not differ from the compressed methane case. As a result, the liquid methane fueled engine shows a lower effectiveness than the compressed methane fueled engine, for the same reason the liquid hydrogen fueled fuel cell has lower effectiveness than the compressed hydrogen fueled fuel cell (that being the greater thermomechanical exergy of the liquid fuel over the gaseous fuel, which is destroyed). The liquid methane engine scenario is disadvantaged in this analysis because no consideration is given to the expected improvement in engine performance when liquid methane (as opposed to compressed methane, see section 5.1.2) is the fuel.

In the future, fully optimized methane fueled vehicles will probably have efficiency somewhere between that of gasoline and methanol fueled vehicles [55]

[3]The actual study [57] used natural gas as the fuel. Because natural gas is largely methane, no distinction between the fuels was made here.

(and maybe even better than methanol), which in turn implies comparable effectiveness. In such a scenario, with the methane engine effectiveness at 0.25, the methane engine pathways have net effectiveness 0.237 and 0.230 for the compressed and liquid fuel respectively. Then, the methane pathways would clearly exceed both of the methanol pathways in net effectiveness. This is directly related to the poor effectiveness (0.409) of methanol production. In fact, the ineffectiveness of this process would preclude further consideration of methanol pathways if effectiveness was the only consideration. It is interesting to note that hydrogen production from methane is almost twice as effective as methanol production from methane.

The liquefaction and compression processes all have relatively high effectiveness. The exergy input as methane, some portion of which is transformed into work in order to accomplish the state change, is generally small in comparison to the chemical exergy of the fuel, driving the effectiveness towards unity. Liquefaction of hydrogen has the lowest effectiveness of these processes. Hydrogen liquefies at a much lower temperature than methane (20 K versus 111 K). The work required for liquefaction was taken as 39 MJ/kg of hydrogen liquefied (78.6 MJ/kgmole). This is within the range given by several researchers [44, 43, 64] and it is high compared to the work required to liquefy methane, 2.5 MJ/kg (40.6 MJ/kgmole) [54].

Figure 6.2 shows the exergy input to each process. This value is related inversely to effectiveness. Exergy enters each process as methane or a methane-derived fuel, either as chemical feedstock or fuel or both. Of that total exergy, only some may be contributed by the product of the previous process. For example, liquefaction of hydrogen requires exergy input in the form of gaseous hydrogen (feedstock), and methane (fuel to produce electricity). The feedstock came from the previous process, however the fuel did not. This consideration leads to net path effectiveness being a weighted product of process effectiveness and exergy input, as previously detailed. The processes having the greatest

path effectiveness require the least exergy input.

6.1.1 Exergy Efficiency

Exergy efficiency and effectiveness provide identical values for all processes examined except those of liquefaction and compression. Figure 6.3 shows the exergy efficiencies for the process in the source to service transformations for each path.

	METHANOL		HYDROGEN		METHANE	
			LIQUID	COMPRESSED	LIQUID	COMPRESSED
PATH	FUEL CELL	S.I. ENGINE	FUEL CELL	FUEL CELL	S.I. ENGINE	S.I. ENGINE
SOURCE TO CURRENCY	.409	.409	.744	.744		
LIQUEFY/ COMPRESS			.161	.210	.186	.217
ON-BOARD FUEL CONDITION	.657					
VEHICLE ENERGY CONVERSION	.539	.278	.521	.545	.150	.151
NET PATH EXERGY EFFICIENCY	.145	.114	.277	.351	.138	.143

Figure 6.3: Exergy efficiency of processes in the source to transportation service pathway.

The hydrogen liquefaction process has an exergy efficiency of 0.161 for a 250 ton/day plant. Hydrogen liquefies at 20 K. The methane liquefaction process has an exergy efficiency of 0.186 for a liquefaction line averaging 1000 ton/day. Methane liquefies at 111 K. Efficiency increases with increasing plant size, so this may account for some of the difference in liquefaction efficiencies. As well,

Bejan [65] has shown that exergy efficiency decreases as the temperature of liquefaction decreases, and has argued that this increase in losses relative to ideal is due to increased internal heat leak through heat exchangers and frame supports. This also serves to increase the difference in the two exergy efficiencies. Again it should be noted that there are no hydrogen liquefaction plants of either 250 ton/day or 36% plant efficiency, so this scenario represents a best case. A hydrogen liquefaction plant of about 66 ton/day has a maximum 25% exergy efficiency, which would give this step an overall exergy efficiency of 0.113 (this includes both liquefaction and the production of electricity for that process). The net path exergy efficiency becomes 0.234, which is still greater than that of any methane or methanol pathway.

The exergy efficiency of the hydrogen compression process works out be 0.210, and that for methane compression is 0.217. These numbers also include electricity generation. Their similarity indicates that the work of compression is about the same for each currency on a per mole basis. The effectiveness figures (0.812 for hydrogen and 0.946 for methane) indicate that the exergy input for compression as a percentage of total exergy gas compressed is much smaller for methane than for hydrogen.

6.2 Emissions

Figure 6.4 shows the exergy of emissions for each step in the source to service pathway, normalized per unit service. The fuel cell pathways have lower total exergy of emissions than the spark ignition engine pathways, which is expected if only because in general they require lower total exergy (and thus mass of methane) input. The compressed hydrogen fuel cell system clearly shows the lowest exergy of emissions: a total of 190 kJ/km. The liquid hydrogen fuel cell system shows the second lowest exergy of emissions.

The exergy of material emissions is been shown distinct from that of heat

	METHANOL		HYDROGEN		METHANE	
			LIQUID	COMPRESSED	LIQUID	COMPRESSED
PATH	FUEL CELL	S. I. ENGINE	FUEL CELL	FUEL CELL	S. I. ENGINE	S. I. ENGINE
SOURCE TO CURRENCY	110 145	140 185	65 5	70 5		
LIQUEFY/ COMPRESS			45 35	20 10	25 30	20 10
ON-BOARD FUEL CONDITION	150 25					
VEHICLE ENERGY CONVERSION	50 40	255 130	45 35	50 35	435 210	435 315
TOTAL PATH EXERGY OF EMISSIONS	310 210	395 315	155 75	140 50	460 240	455 325
TOTAL EXERGY OF EMISSIONS	520	710	230	190	700	780

Figure 6.4: Emission exergy from each processes in the source to transportation service pathway, with methane as the sole exergy source (kJ/km). Exergy of material emissions is shown in the top half of the box, heat emission exergy is shown in the bottom half of the box.

emissions. Material emissions carry both chemical and thermomechanical exergy. Heat emissions do little work on the environment, but do result in increased entropy. On a global scale this has little effect because entropy is continuously removed from the planet by radiation. However, on a local scale heat emissions may have significant impact. All routes show lower exergy of heat emissions than material emissions.

The total exergy of emissions varies between 10% and 20% of the total exergy input to the pathway, with the fuel cell systems producing a lower percentage exergy of emissions. The methane spark ignition engine systems have almost all of the total path emission exergy coming from the vehicle itself. The methanol

engine system shows about half the emission exergy originating at stationary sources and half coming from the vehicle. The fuel cell systems show that along the pathway, more emission energy originates from processes occurring at stationary sites than originates from mobile sources. If currency production, liquefaction, and compression plants could develop technologies to reduce their emission exergy, for example by collecting carbon dioxide produced by combustion and/or reforming, then a high exergy by-product would result (the emission would be transformed into a potentially valuable commodity). In such a case the emission exergy of each pathway would be reduced, and in fact the emission exergy becomes by-product exergy, and can be considered a credit to the process. It is much more difficult to collect emissions from mobile sources.

The pathways are ranked in order of increasing emission exergy and of increasing exergy input in Table 6.1. Both optics indicate the compressed hydrogen fuel cell pathway is optimal. The rankings are similar in that the hydrogen pathways precede any of the other pathways, and the fuel cell pathways precede the engine pathways. It is expected that a spark ignition engine developed solely for methane fuel (for example with an optimized combustion chamber shape) would perform better, reducing the exergy of consequent emissions.

Table 6.1: Routes for Methane Sourced Transportation Services, in Order of Increasing Exergy of Emissions and of Increasing Total Exergy Input

Pathway	Exergy of Emissions (kJ/km)	Pathway	Exergy Input (kJ/km)
C–H_2, Fuel Cell	190	C–H_2, Fuel Cell	1730
L–H_2, Fuel Cell	230	L–H_2, Fuel Cell	2175
CH_3OH, Fuel Cell	520	CH_3OH, Fuel Cell	4130
L–CH_4, Engine	700	C–CH_4, Engine	4200
CH_3OH, Engine	710	L–CH_4, Engine	4350
C–CH_4, Engine	780	CH_3OH, Engine	5270

The mass of carbon dioxide and water emitted throughout each pathway

are shown in Figure 6.5. Carbon dioxide and water are products of methane combustion, which provides process heat and electricity. Carbon dioxide is also released in the steam methane reforming process. Carbon dioxide has been identified as a significant contributor to the greenhouse effect and global climatic change. The total mass of carbon dioxide from each pathway is directly related to the total mass of the exergy source methane required by that pathway. The hydrogen fuel cell pathways thus produce the least, while the methanol pathways produce the most carbon dioxide. The same pattern is seen with mass of water emitted from the pathways. The greater effectiveness of the fuel cell pathways reduces the exergy input requirement and thus the mass of methane input required to provide the unit service, resulting in the lowest mass of emissions.

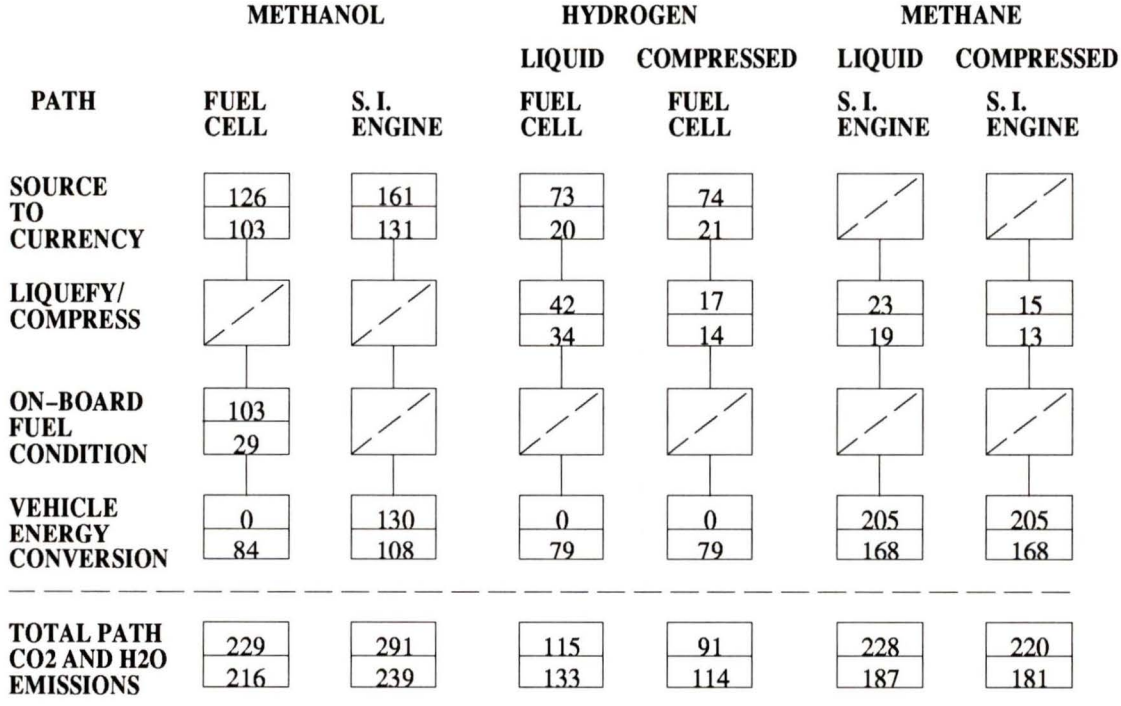

Figure 6.5: Mass of carbon dioxide (top half of box) and water (bottom half of box), from each process in the source to transportation service pathway, with methane as the sole exergy source (g/km).

It is a misconception that the hydrogen fuel cell pathways will result in a world flooded by water from emissions. In fact, to perform the same city driving service it is clear that less water vapour is produced, both by the vehicle itself and throughout the entire pathway than when the same service is provided via methane or methanol pathways.

Chapter 7

Concluding Comments

If the premise that natural gas (and thereby methane) will have an increasingly important role as an energy source in the future is accepted, then it is necessary to consider the opportunities for increasingly efficient and low polluting technologies which may arise. These opportunities with respect to providing the service transportation have been investigated and analyzed from two perspectives based on the second law of thermodynamics.

The energy conversion steps in each pathway have been examined for six possible routes, beginning with methane as the energy source and ending with the energy service one kilometer of city driving. Pathways were compared assuming that all vehicles with a fuel cell power train had identical weight and drag characteristics (those of an *average* passenger car), and these features were similar to those in engine powered vehicles. As a result, fuel storage and vehicle range effects have been neglected. Source extraction, currency distribution, economics, and risk have also been neglected. Under these conditions, the following can be concluded:

- The compressed hydrogen, fuel cell pathway is optimal from an efficiency perspective, followed by the liquid hydrogen, fuel cell pathway.

- The hydrogen fuel cell pathways produce both the least carbon dioxide and the least water of the pathways considered. Clearly, hydrogen technologies

will not flood the world with water emissions. As well, these pathways contribute least to atmospheric carbon dioxide build-up.

- The hydrogen fuel cell pathways exhibit the lowest exergy of emissions of the pathways considered. If exergy of emissions is interpreted as an indicator of potential for environmental impact, then these pathways are more coherent with natures' fluxes than those pathways involving carbon energy currencies.

- The methane pathways result in less carbon dioxide produced than the methanol pathways.

- The low exergy efficiency of hydrogen and methane liquefaction and compression indicates that process irreversibilities are large in relation to process exergy inputs. Conventional technology has been considered. It is likely that any breakthroughs in these areas will be a result of new technologies.

- The low efficiency of spark ignition engines compared to solid polymer fuel cells indicates that the fuel cell more closely approximates a reversible process, and this makes it a better method of energy conversion.

- In order for the methanol fuel cell route to become competitive with the other fuel cell routes from an efficiency perspective, substantial improvements in methanol production are required.

- Emission exergy has given results not inconsistent with those expected from an indicator of environmental impact. Consequently, exergy of emissions appears to have some relation to environmental impact. Caution must be used in interpreting this, as emission exergy varies with the reference environment chosen. Furthermore, emission exergy can not be considered the sole indicator of environmental impact because impact on the biosphere is not accounted for.

It has been observed that more efficient systems are cheaper over the long term, and in fact that 'Cleaner is Cheaper'[1]. More comprehensive studies, such as those of DeLuchi [66], have found some of the same broad results: that the energy currency methane looks better than methanol in terms of emissions and that compressed methane offers slightly greater benefits than liquid methane.

7.1 Opportunities for Future Work

This study falls short of being comprehensive. Major considerations such as the exergy requirements of fuel storage and distribution systems, effects of fuel tank weight on vehicle performance and range, risk, and economics of these systems have not been addressed. As well, only one duty cycle has been considered: that of the urban automobile. The vehicular exergy conversion technology effectiveness is related to load, so effectiveness over bus, locomotive, submersible and other duty cycles would vary.

Analyses of the liquefaction and compression processes in this study was general; based on end states and work requirements. Thorough exergy analyses of some methane liquefaction cycles has been performed [67] showing the irreversibility of heat exchange and compression processes. As well, second law analyses of large scale (250 ton/day) hydrogen liquefaction cycles are available [44, 43]. Opportunities to examine cycles for smaller plants and non-conventional processes exist. Some interesting studies concerning the effects of variation in inlet and delivery pressures on compression power have been done [50]. This study assumed the same inlet conditions for hydrogen and methane (as detailed in their respective chapters), and a specific delivery pressure, for the purpose of defining one representative effectiveness value for the compression processes. The compression work required for both hydrogen and natural gas (88% methane) have been compared and explained [68]. Although

[1] An encapsulation credited to the late Ed Schmidt.

some studies have been done [69], there remains room for investigation of compressor performance in the field.

Most studies of on-board methanol reformers have assumed an internal combustion engine downstream to receive the reformer products and to provide process heat. This thesis has adapted the operating characteristics of these reformers best suited for a fuel cell system. A detailed second law analysis of a methanol reformer designed to produce hydrogen for a fuel cell could be useful.

Bibliography

[1] M. J. Moran and H. N. Shapiro. *Fundamentals of Engineering Thermodynamics.* John Wiley and Sons, New York, 1988.

[2] J. Szargut. International progress in second law analysis. *Energy*, 5:709–718, 1980.

[3] K. Katoh, Y. Imamura, and T. Inoue. Development of methanol lean burn system. Technical Report 860247, SAE, 1986.

[4] J. Alson and T. M. Baines. Emissions and energy efficiency characteristics of methanol fuelled engines and vehicles. In *Nonpetroleum Vehicular Fuels III Symposium Papers*, pages 399–431. Institute of Gas Technology, October 1983.

[5] H. Menrad, W. Bernhardt, and G. Decker. Methanol vehicles of Volkswagen - A contribution to better air quality. Technical Report 881196, SAE, 1988.

[6] Taylor, Alderson, et al. Technical and economic assessment of methods for the storage of large quantities of hydrogen. *International Journal of Hydrogen Energy*, 11(1):5–22, 1986.

[7] Sulzer Burckhardt. C3H series reciprocating compressors. Brochure.

[8] C. S. Weaver. Natural gas vehicles - a review of the state of the art. Technical Report 892133, SAE, 1989.

[9] B. C. Research, Physical Technology Division. Exhaust emission characteristics of natural gas fuelled vehicles operating at lean air/fuel ratios. Technical report, Prepared for Energy, Mines and Resources Canada, Transportation Energy Division, Vancouver, British Columbia, 1986.

[10] T. G. Adams. Ford's experience with dedicated compressed natural gas powered vehicles. In *Gaseous Fuels for Transportation I*, pages 759–770, 1986.

[11] F. L. Fischer. Introduction of a commercial system for liquid methane vehicles. In *Nonpetroleum Vehicular Fuels III Symposium Papers*, pages 125–142. Institute of Gas Technology, October 1983.

[12] A. Golovoy and J. Braslaw. On-board storage and home refueling options for natural gas vehicles. Technical Report 830382, SAE, 1983.

[13] G. B. O'Neal. Improving the efficiency of a spark-ignition engine for natural gas fuel - phase II status report. In *Proceedings of the Twenty-Second Automotive Technology Development Contractors' Coordination Meeting*, March 1985.

[14] B. C. Hydro. Proposed Sasamat natural gas storage plant project report. Technical report, Gas Engineering Division, December 1981.

[15] D. S. Scott and H. H. Rogner. Natural gas: Staple energy source of the 21^{st} century. Technical report, Presented at the Canadian Gas Association 6^{th} National Technical Conference, Vancouver, BC, February, 1991.

[16] C. Marchetti and N. Nakicenovic. The dynamics of energy systems and the logistic substitution model. Technical Report RR-79-13, International Institute for Applied Systems Analysis, 1979.

[17] D. S. Scott and Wolf Häfele. The coming hydrogen age: Preventing world climatic disruption. *International Journal of Hydrogen Energy*, 15(10):727 – 737, 1990.

[18] D. S. Scott et al. Hydrogen – National mission for Canada. Technical Report Cat. No. M27-86/1987E, ISBN 0-662-15544-0, Report of the Advisory Group on Hydrogen Opportunities, Supply and Services Canada, June 1987.

[19] Energy balances of OECD countries 1987-1988. International Energy Agency, Paris, France, 1990.

[20] J. Szargut. Minimization of the consumption of natural resources. *Bulletin de L'Academie Polonaise des Sciences, Serie des Sciences Techniques*, 26:611–615, 1978.

[21] R. A. Gaggioli and P. J. Petit. Use the second law, first. *Chemtech*, 7:496–506, 1977.

[22] M. W. Chase Jr., C. A. Davies, et al. *JANAF Thermochemical Tables.* Volume 14, American Chemical Society and American Institute of Physics for the National Bureau of Standards, 3rd Edition, 1985.

[23] M. J. Moran. *Availability Analysis: A Guide to Efficient Energy Use.* Prentice Hall, Englewood Cliffs, NJ, 1982.

[24] T. J. Kotas. *The Exergy Method of Thermal Plant Analysis.* Butterworths, Toronto, 1985.

[25] M. A. Rosen. *The Development and Application of a Process Analysis Methodology and Code Based on Exergy, Cost, Energy and Mass.* PhD thesis, Dept. of Mechanical Engineering, University of Toronto, Toronto, 1986.

[26] P. Crane, D. S. Scott, and M. A. Rosen. Exergy of emissions as a measure of potential for environmental impact. In T. N. Veziroğlu and P. K. Takahashi, editors, *Hydrogen Energy Progress VIII, Proceedings of the 8th World Hydrogen Energy Conference*, volume 1, pages 163 – 171. Pergamon Press, 1990.

[27] R. Kummel and U. Schüssler. Heat equivalents of noxious substances: A pollution indicator for environmental accounting. *Ecological Economics*, 1990.

[28] W. C. Reynolds. *Thermodynamic Properties in SI.* Department of Mechanical Engineering, Stanford University, 1979.

[29] R. D. Goodwin. Methanol thermodynamic properties from 176 to 673 K at pressures to 700 bar. *J. Phys. Chem. Ref. Data*, 16(4):799–892, 1987.

[30] H. M. Roder, R. D. McCarty, and W. J. Hall. Computer programs for thermodynamic and transport properties of hydrogen (Tabcode–II). Technical Report Technical Note 625, U. S. Department of Commerce, National Bureau of Standards, Boulder, Colorado, October, 1972.

[31] I.M. Alatiqi, A. M. Meziou, and G. A. Gasmelseed. Modelling, simulation and sensitivity analysis of steam-methane reformers. *International Journal of Hydrogen Energy*, 14(4):241–256, 1989.

[32] S. Fujimoto, H. Ishihara, and S. Tsuruno. A study of a steam reformer for methanol. *JSME International Journal*, 30(267):1437–1442, 1987.

[33] J. Finegold, M. Karpuk, J. McKinnon, and R. Passamaneck. Demonstration of dissociated methanol as an automotive fuel: System performance. In *Proceedings of the 1981 Annual Meeting, American Section of the International Solar Energy Society*, volume 4.1, pages 221–224, 1981.

[34] K. Sjostrom and G. Landqvist. Onboard hydrogen generation for hydrogen injection into internal combustion engines. Technical Report 810348, SAE, 1981.

[35] F. L. Kester, A. J. Konopka, and E. H. Camara. On-board steam reforming of methanol to fuel the automotive hydrogen engine. In *Intersociety Energy Conversion Engineering Conference 1975 Record*, pages 1176–1183, 1975.

[36] G. E. Voecks, S. Dawson, and J. Houseman. Operation of a catalytic methanol decomposition reactor for vehicular use. In *Proceedings, 4th International Symposium on Alcohol Fuels Technology*, Brazil, October 1980.

[37] J. Houseman and D. J. Cerini. Onboard hydrogen generation for automobiles. In *11th Intersociety Energy Conversion Engineering Conference Proceedings*, pages 6–16, 1976.

[38] G. K. Piotrowski and J. D. Murrell. Phase I testing of Toyota lean combustion system (methanol). Technical Report EPA/AA/CTAB/87-02, U. S. Environmental Protection Agency, January, 1987.

[39] K. Darrow, N. Biederman, and A. Konopka. Commodity hydrogen from off-peak electricity. *International Journal of Hydrogen Energy*, 2:175–187, 1977.

[40] J. A. Barclay. A review of magnetic heat pump technology. In *International Energy Conversion Engineering Conference*, August 1990.

[41] J. A. Waynert, T. J. DeGregoria, R.W. Roster, and J. A. Barclay. Magnetic heat pumps for hydrogen liquefaction. In *ASME Winter Annual Meeting, Industrial Heat Pumps Session*, December 1989.

[42] J. A. Barclay. Magnetic refrigeration: A review of a developing technology. In *Cryogenics Engineering Conference*, June 1987.

[43] D. Dini and G. Dini. Thermochemical computation of hydrogen liquefaction plants. In *Hydrogen Energy Progress VIII, Proceedings of the 8th World Hydrogen Energy Conference*, pages 873–890, 1990.

[44] C. R. Baker and R. L. Shaner. A study of the efficiency of hydrogen liquefaction. *International Journal of Hydrogen Energy*, 3:321–334, 1978.

[45] T. R. Strobridge. Cryogenic refrigerators – an updated survey. Technical report, Cryogenics Division, National Bureau of Standards, June, 1974.

[46] L. A. Poch, J. L. Gillette, and B. A. Hedman. Regional application of natural-gas-fired combined-cycle power generation. In W. D. Jackson, editor, *24th Intersociety Energy Conversion Engineering Conference Proceedings*, volume 4, pages 1795–1800, August, 1989.

[47] K. Prater. The renaissance of the solid polymer fuel cell. *Journal of Power Sources*, 29:239–250, 1990.

[48] K. Prater. Ballard Power Systems, Personal Communciations, between January 1990 and February 1991.

[49] R. Ewald and M. Kesten. Cryogenic equipment of liquid hydrogen powered automobiles. In *Advances in Cryogenic Engineering*, volume 35, pages 1777–1796. Plenum Press, 1990.

[50] P. Magistris and V. Bellini. Compression of natural gas for automotive service: Economic and technical aspects. *Quaderni Pignone*, 34:33–38, 1982.

[51] G. Walker. Design guidelines for large stirling cryocoolers. *Cryogenics*, pages 113–114, February 1983.

[52] R. Dunbar, W. Ellison, and G. Walker. Gas-fired natural gas liquefier for vehicle fuel. In R. W. Fast, editor, *Advances in Cryogenic Engineering.*

Plenum Press, New York, 1990.

[53] L. Kniel. Energy systems for LNG plants. *Chemical Engineering Progress*, 69(10):77–84, 1973.

[54] C. H. Gatton. *Liquefied Natural Gas Technology and Economics.* Noyes Development Corporation, New Jersey, 1967.

[55] M. A. DeLuchi, R. A. Johnston, and D. Sperling. Methanol vs natural gas vehicles: A comparison of resource supply, performance, emissions, fuel storage, safely, costs, and transitions. Technical Report 881656, SAE, 1988.

[56] J. B. Heywood. *Internal Combustion Engine Fundamentals.* McGraw Hill, New York, 1988.

[57] T. E. S. Limited. Gas powered vehicle evaluation program. Technical report, Prepared for Transport Canada Road Safety Branch, March 1982.

[58] Jean de Grasse. Centra Gas, personal communication, Victoria, October, 1990.

[59] Y. Kimbara, S. Katsumata, T. Ichimiya, M. Kan, and S. Kondo. Development of Toyota electronically controlled natural gas vehicle. In *Gaseous Fuels for Transportation I*, pages 771–790, 1986.

[60] M. A. DeLuchi. Hydrogen vehicles: An evaluation of fuel storage, performance, safety, environmental impacts, and cost. *International Journal of Hydrogen Energy*, 14(2):81–130, 1989.

[61] G. R. Slemon and A. Straughen. *Electric Machines.* Addison-Wesley Publishing Co., Don Mills, Ontario, 1982.

[62] R. D. Fleming and G. B. O'Neal. Potential for improving the efficiency of a spark ignition engine for natural gas fuel. Technical Report 852073, SAE, 1985.

[63] M. R. Swain, R. Maxwell, M. N. Swain, K. Bedsworth, R. Adt, and J. Pappas. Methane fueled engine performance and emissions characteristics. In *18th Intersociety Energy Conversion Engineering Conference Proceedings*, pages 626–629. American Institute of Chemical Engineers, 1983.

[64] G. Walker, G. Reader, and O. R. Fauvel. Small scale liquefaction of hydrogen. In *Hydrogen Energy Progress VIII, Proceedings of the 8th World Hydrogen Energy Conference*, pages 891–902, 1990.

[65] A. Bejan. *Advanced Engineering Thermodynamics.* John Wiley and Sons, 1988.

[66] M. A. DeLuchi. State–of–the–art assessment of emissions of greenhouse gases from the use of fossil and nonfossil fuels, with emphasis on alternative transportation fuels. Technical report, Division of Environmental Studies, University of California, Davis (forthcoming in revised form from Argonne National Labs.), 1990.

[67] C. H. Chiu and C. L. Newton. Second law analysis in the cryogenic processes. Technical Report 79-0055, Air Products and Chemicals, Inc., Allentown, PA, August, 1989.

[68] J. S. Wallace. A comparison of compressed hydrogen and CNG storage. *International Journal of Hydrogen Energy*, 9(7):609–611, 1984.

[69] B. C. Research Applied Physics and Engineering Division. CNG compressor operations monitoring. Technical report, Prepared for Deparment of Energy, Mines and Resources Canada, April 1987.

[70] C. Bowman. President, Alberta Research Council, Personal Communciation, June 1991.

[71] M. A. Warner-Selph and J. DeVita. Measurements of toxic exhaust emissions from gasoline-powered light-duty vehicles. Technical Report 892075, SAE, 1989.

[72] Society of Automotive Engineers, Warrendale, PA. *SAE Handbook*, 1989.

Appendix A

Gasoline – The Current Situation

This thesis has examined the efficiency of and emission exergy arising from different methods of using methane to provide the transportation service. For the purposes of comparison, the production of gasoline from crude oil and the use of gasoline in automobile engines is investigated here.

A.1 Production of Gasoline from Crude Oil

It is difficult to identify the energy required to produce specific products in a petroleum refinery due to the integrated nature of petroleum refining. The analysis of this thesis does not attempt such an allocation. Rather, net refinery efficiency is taken to be 85% [70]. This is the ratio of desired energy products out (such as gasoline and other distillates) to process energy input plus other products out (those of little value such as char and other heavy ends). A typical refinery process fuel mix is shown in Table A.1. Virtually all of the material emissions from a refinery are a result of fuel combustion for process energy. The emission exergy of these stack gases can be calculated, however, the exergy of heat emissions from a refinery are not as readily determined.

Several simplifying assumptions are made. In order to calculate the chemical exergy of gasoline and the stoichiometric oxygen requirement for gasoline

Table A.1: Fuels Used to Provide Process Energy in a Refinery[1]

Energy Source	Contribution to Process Energy (%)	Mass of Carbon per Mass of Fuel
Diesel	0.68	0.855
Residual Oil	2.95	0.858
LPG	1.08	0.817
Natural Gas	28.94	0.749
Coke	17.04	0.9
Refinery Gas	49.32	0.778

[1]From DeLuchi [66]

combustion, gasoline is approximated as a mixture of 31% benzene and 69% octane by mass. This composition is chosen by using the chemical formula $C_nH_{1.84n}$, given by [66], and by considering the composition to be primarily saturates (such as octane) and aromatics (which contain at least a benzene ring). The fuels which are burned to provide process energy are diesel, residual oil, propane, natural gas, coke, and refinery gas. The exergy of each fuel is taken as its higher heating value. This is also assumed for the exergy of crude oil. This is a reasonable approximation as the energy grade of fossil fuels is approximately unity. It is assumed that the electricity consumed was generated from natural gas combusted in 40% excess air. All fuels are assumed to consist of carbon and hydrogen only, with the difference being the atomic H:C ratio. The mass of carbon per unit mass fuel is also shown in Table A.1.

The refinery efficiency of 85% is taken to be the exergy efficiency (and also effectiveness) of gasoline production. For every energy unit of gasoline produced, 0.059 energy units of process energy and 1.118 energy units of crude oil feedstock are required. The exergy of material emissions is less than 1% of the total fuel exergy input to the process. 0.061 g of carbon dioxide and 0.074 g of water are emitted per kJ of process energy based on the above fuel mixture.

A.2 Currency to Service Transformation

A fuel consumption of about 71.14 g/km (corresponding to 25 mpg, city) is taken as representative for the average light duty vehicle. This value is consistent with that shown in some literature [71]. This translates to an exergy input of 3255 kJ/km (based on the previously noted formulation for gasoline). Effectiveness of the engine is found by assuming that the total exergy output over the duty cycle from the fuel cell is the same as the the total exergy output from the engine. Engine effectiveness is 0.184. Engine emissions are also taken from [71]. Hydrocarbon emissions are assumed to consist entirely of unburnt fuel (i.e., benzene and octane in their respective proportions). NO_x emissions are assumed to be 25% (by mass) nitrogen dioxide and the rest nitrogen monoxide. Heat emissions are taken to be at 80°C as usual for water cooled engines. This leads to a material emission exergy of 390 kJ/km and a heat emission exergy of 305 kJ/km. A total of 220 g/km of carbon dioxide and 85 g/km of water are produced. These exergy and material flows are shown in Figure A.1.

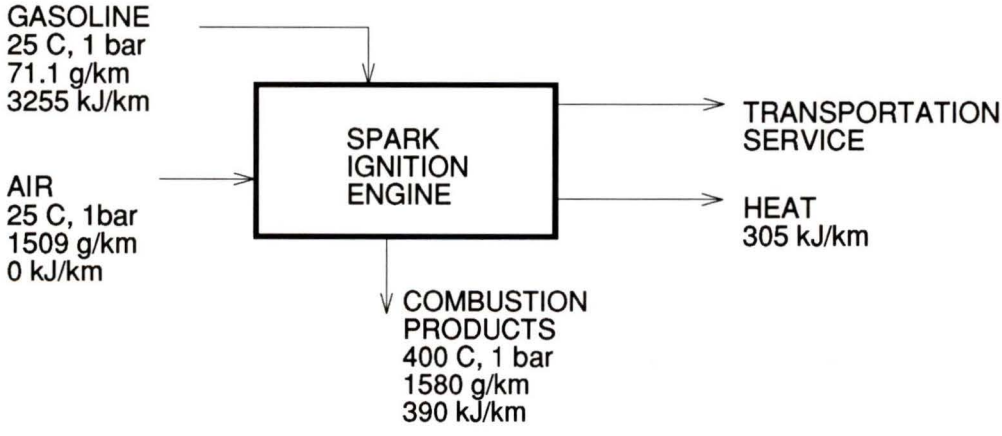

Figure A.1: Exergy and material flows for a gasoline fueled spark ignition engine.

A.3 Net Path Effectiveness and Emissions: Comparison with Other Routes

Figures A.2 and A.3 compare the pathways for methane use in transportation to the gasoline from crude oil pathway in terms of effectiveness and total exergy input. The gasoline net path exergy efficiency of 0.156 is higher than that for the routes involving methane or methanol as the energy currency. Only the hydrogen routes are more efficient. The gasoline engine effectiveness is 0.184, which is better than that for methane fueled engines (around 0.15 in their rudimentary state of development) but not nearly as good as that for the methanol fueled engine (which has been highly engineered and shows an effectiveness of 0.278). Again the low efficiency of methanol production reduces its ability to compete. The total exergy input to the gasoline pathway is 3830 kJ/km, in the form of crude oil.

It should be noted that this analysis does not include consideration of the extraction of crude oil nor of the extraction and desulfurization of methane. If these processes were included, the pathways involving methane as the sole exergy source could look better compared to gasoline, both in terms of efficiency and emissions, depending on the sources of petroleum and natural gas.

The total exergy of emissions from this pathway is not determined. Although the emissions from fuel combustion for process energy are readily determined (with the simplifying assumptions noted previously), heat emissions are not. The exergy of material emissions from refining is 12.96 kJ/km. The engine produces a total emission exergy of 695 kJ/km, of which 390 kJ/km is associated with material emissions and the rest is emitted as heat. The total emission exergy (on the vehicle energy conversion line, Figure A.4) is greater than that for the methanol fueled engine and the liquid methane fueled engine, but less than that for the compressed methane fueled engine. Figure A.5 shows the carbon dioxide and water produced from each pathway, including the gasoline

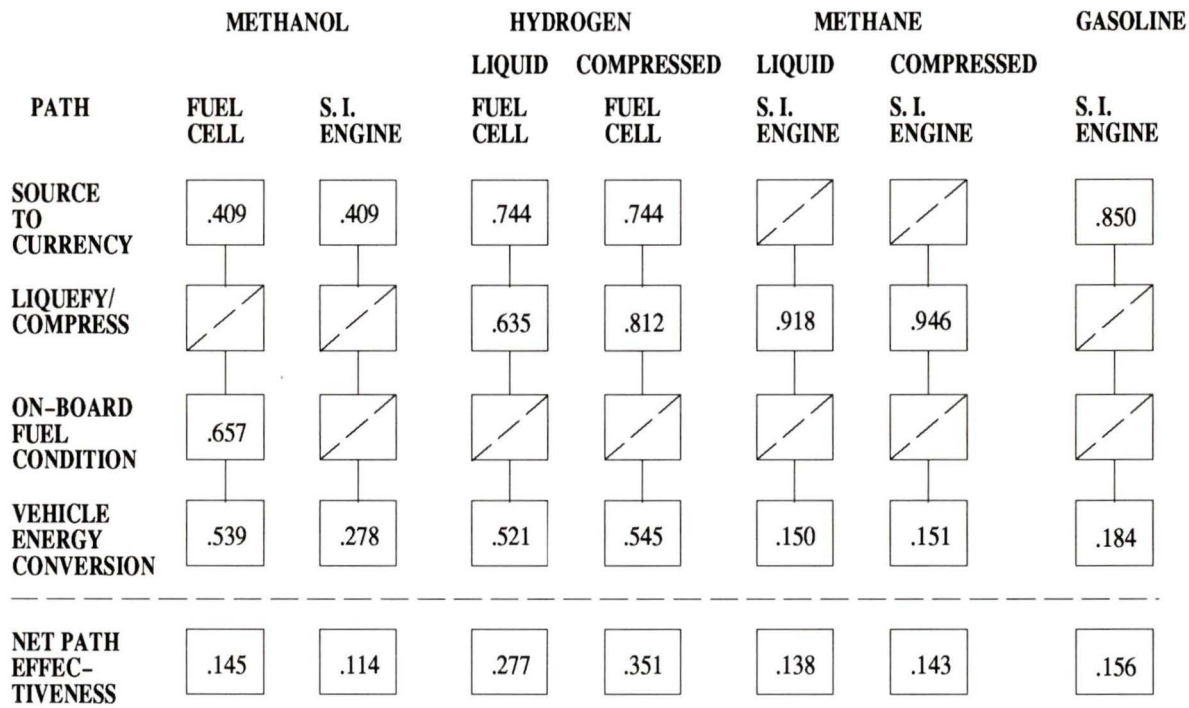

Figure A.2: Effectiveness of technical pathways for methane sourced transportation fuels, with gasoline from crude oil for comparison.

route. The total carbon dioxide output (220 g/km) from the gasoline pathway is comparable to that output from the methane pathways and the methanol fuel cell pathway. It is lower than that from the methanol spark ignition engine pathway. Although the methane fueled engine requires more exergy, methane has a lower atomic carbon to hydrogen ratio than gasoline. As a result, more exergy can be supplied with less carbon in the fuel.

PATH	METHANOL		HYDROGEN		METHANE		GASOLINE
			LIQUID	COMPRESSED	LIQUID	COMPRESSED	
	FUEL CELL	S.I. ENGINE	FUEL CELL	FUEL CELL	S. I. ENGINE	S. I. ENGINE	S. I. ENGINE
SOURCE TO CURRENCY	4130	5270	1385	1440			3830
LIQUEFY/ COMPRESS			1820	1360	4350	4200	
ON-BOARD FUEL CONDITION	1690						
VEHICLE ENERGY CONVERSION	1110	2155	1155	1105	3995	3975	3255
TOTAL PATH EXERGY INPUT	4130	5270	2175	1730	4350	4200	3830

Figure A.3: Exergy required to provide the transportation service, with gasoline from crude oil for comparison (kJ/km).

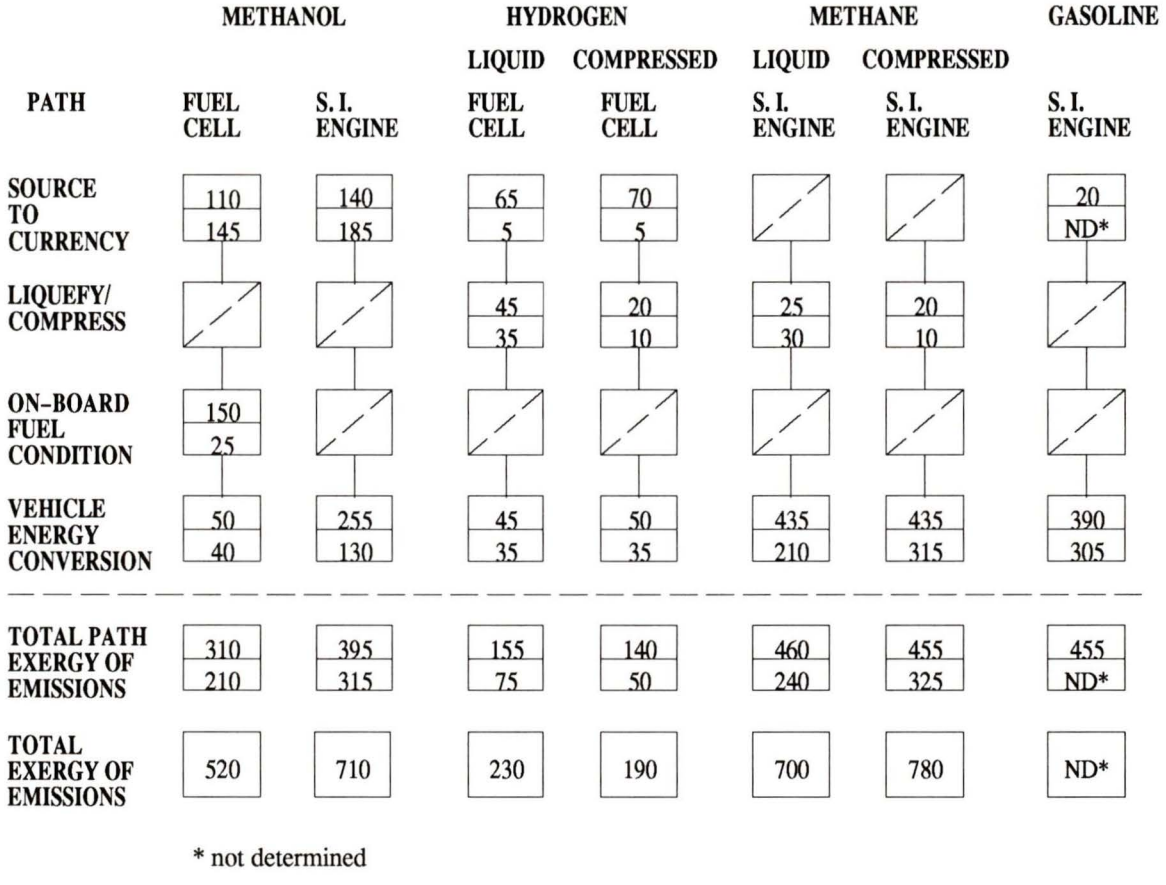

Figure A.4: Emission exergy from process in the source to service pathway, with gasoline from crude oil for comparison. Exergy of material emissions is shown in the top half of the box, heat emission exergy is shown in the bottom half of the box (kJ/km).

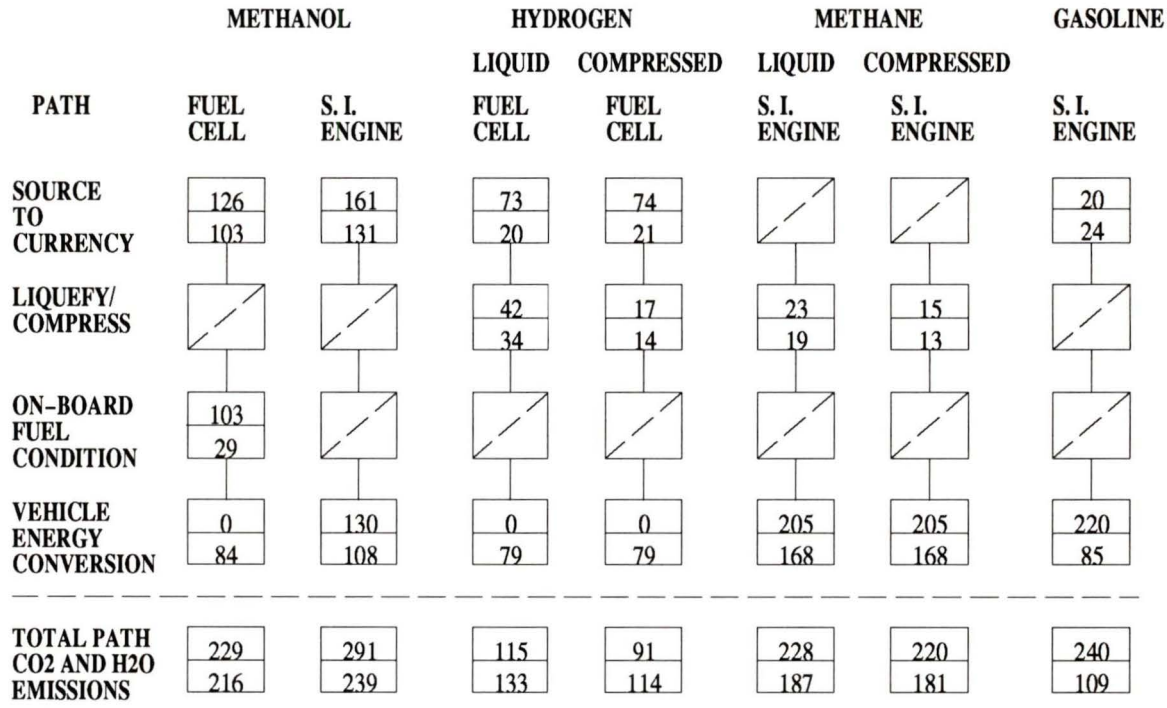

Figure A.5: Mass of carbon dioxide (top half of box) and water (bottom half of box), from each process in the source to transportation service pathway, with gasoline from crude oil for comparison (g/km).

Appendix B

Duty Cycles: City Driving

This thesis is concerned with the use of methane as an energy source for transportation applications, particularly automobiles used for urban driving. It is necessary to define this transportation service in terms of an energy requirement, in order to obtain exergy efficiencies. The load on a fuel cell power train must be determined. The duty cycle of a vehicle is defined as a load versus time profile, characteristic of some service. For light duty vehicles, fuel economy and exhaust emissions are generally determined using one of the Society of Automotive Engineers (SAE) recommended dynamometer driving schedules. These provide second–by–second definitions of vehicle speed versus time, which can be simulated using a dynamometer and suitable vehicle test bed. The two urban cycles pertinent in this thesis are the 1975 Federal Test Procedure (FTP) and the Environmental Protection Agency Urban Dynamometer Driving Schedule (UDDS)[1]. The FTP actually consists of the entire UDDS plus the first 505 seconds of the UDDS repeated. These driving schedules in terms of speed versus time are shown in Figure B.1 and Figure B.2.

The road load force on a vehicle is a function of vehicle velocity and is given by

$$- M_e \frac{dV}{dt} = f_\circ + f_2 V^2 \tag{2.1}$$

[1]The FTP was used in [38] for the methanol vehicle fuel economy and emissions tests, but [57] used the UDDS for the methane fueled vehicle tests.

where M_e is the total vehicle mass plus the effective mass of rotating components (wheel, tires etc.), and $f_\circ$ and f_2 are force coefficients. These force coefficients are given by

$$f_\circ = \mu_\circ W \tag{2.2}$$

$$f_2 = \mu_\circ \mu' W + 0.5\rho C_D A \tag{2.3}$$

where $\mu_\circ$ is the dimensionless coefficient of rolling resistance, μ' is the velocity coefficient of rolling resistance, W is the weight of the vehicle including 136 kg payload of driver and baggage, ρ is the density of air, C_D is the coefficient of drag for the vehicle, A is the vehicle frontal area. A power–velocity equation is derived from the force velocity equation yielding

$$P = f_\circ V + f_2 V^3 \tag{2.4}$$

The coefficients in the force–velocity equation (2.1) were found from coast-down measurements[2] for an *average* automobile, where the average automobile was defined from a sample size of four. These four automobiles were produced by different manufacturers and were not necessarily of the same model year. The four vehicles were chosen as representative of those used in in the actual emissions tests for methanol and methane fueled vehicles. The average values of $f_\circ$ and f_2 were 0.0166 and 0.568 respectively.

Using equation 2.4, the velocity versus time FTP can be transformed into a power versus time road load on the vehicle wheels, which must be met by the fuel cell drive train. The power versus time chart corresponding to the UDDS is shown in Figure B.3. During periods of deceleration and rest, the fuel cell will be operating at some minimal power output, primarily to maintain air compressor and cooling water functions so that it will keep itself running. Regeneration was not considered. This minimal power output was set at 2.8 kW.

[2]It was assumed that both coastdown measurements and exhaust emissions and fuel economy tests followed SAE guidelines as published in the SAE Handbook, Volume 3: Engines, Fuels, Lubricants, Emissions, and Noise [72].

When the fuel cell simulation was run through the FTP and UDDS power versus time schedules, it was found that the UDDS gave slightly lower fuel consumption results than the FTP. The fuel consumption and emissions found using each of the two duty cycles were averaged (added together and divided by two) to determine a representative performance for the hydrogen fueled fuel cell systems. The final transportation service was normalized on the basis of one kilometer of city driving.

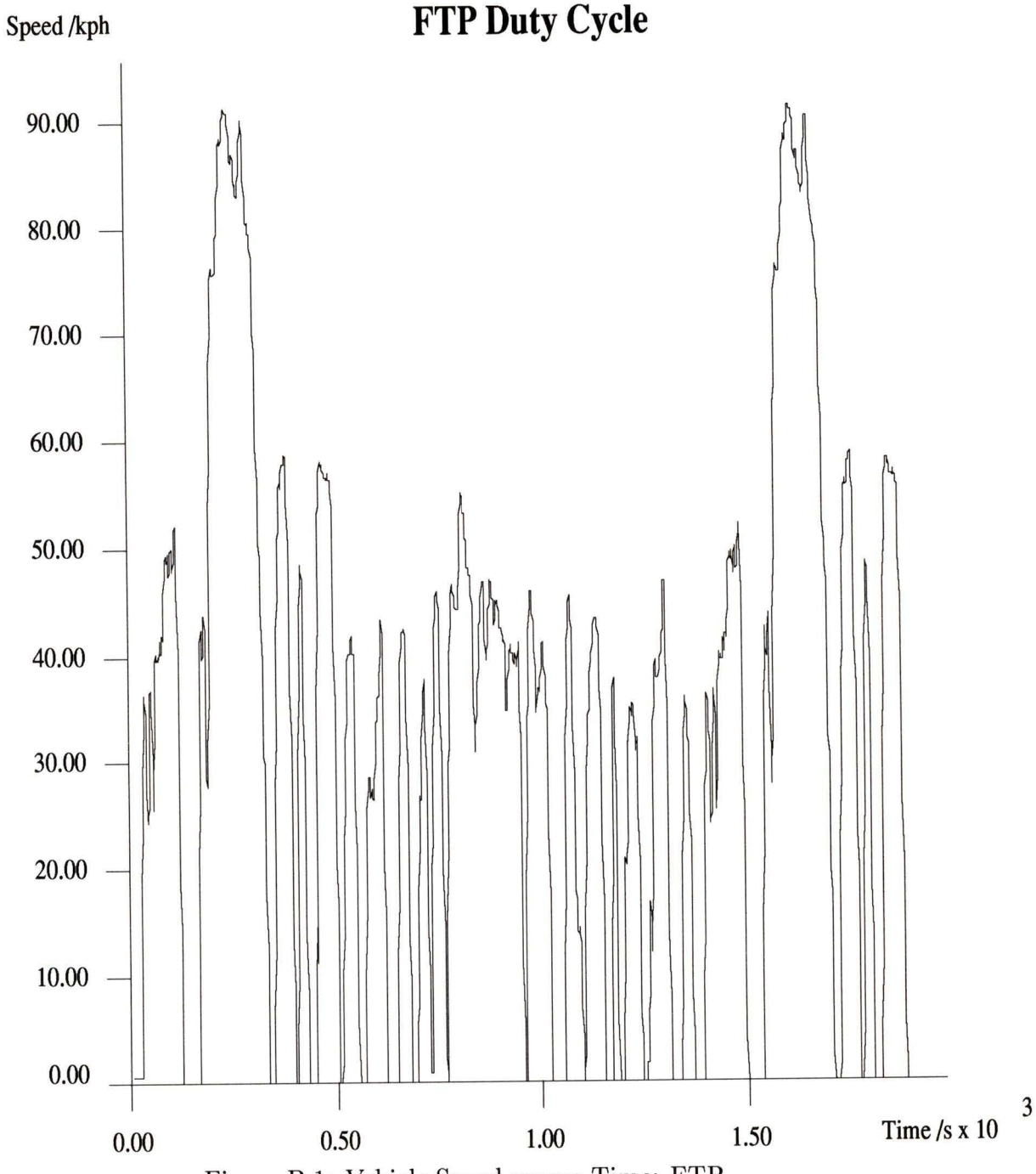

Figure B.1: Vehicle Speed versus Time: FTP.

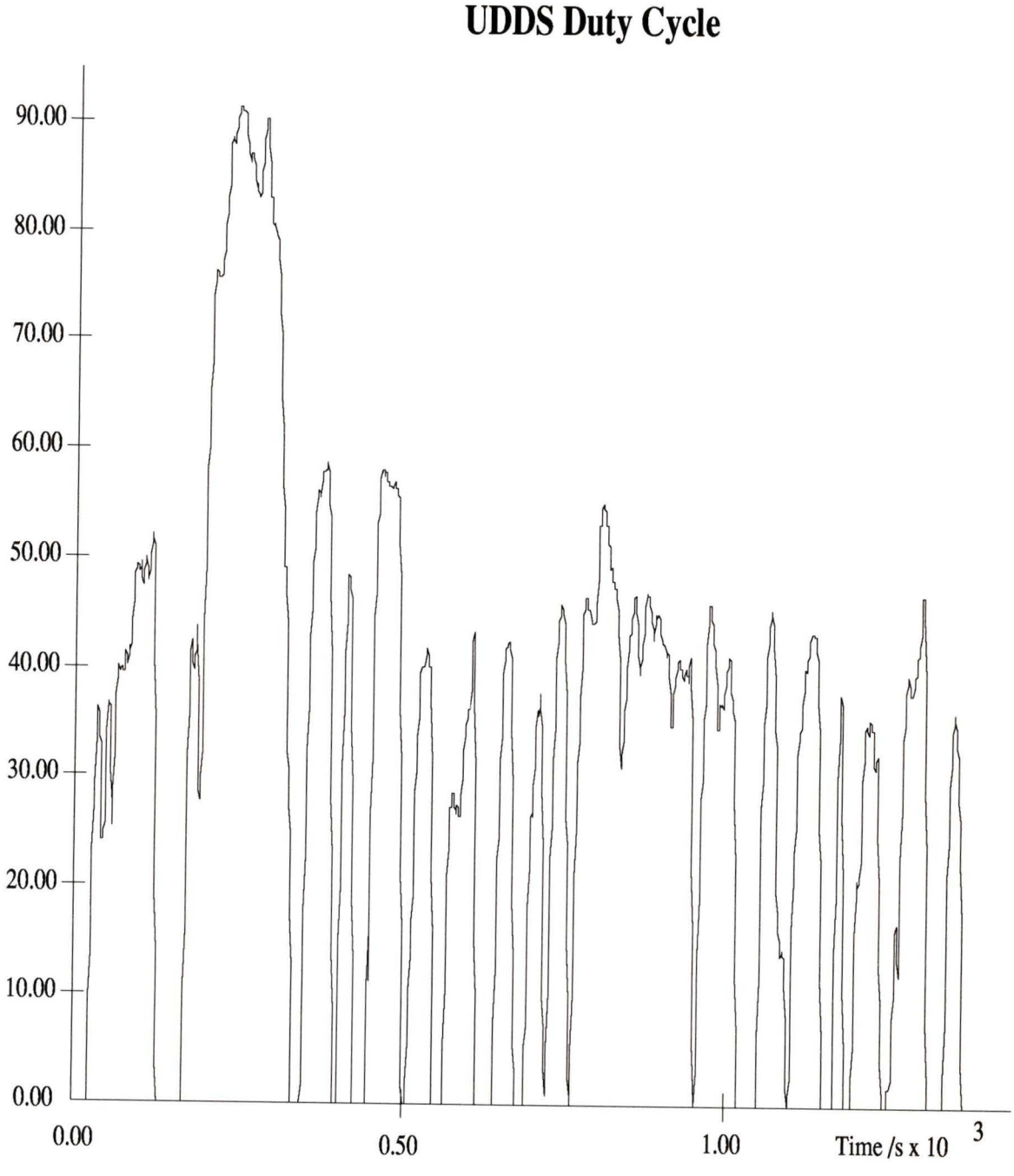

Figure B.2: Vehicle Speed versus Time: UDDS.

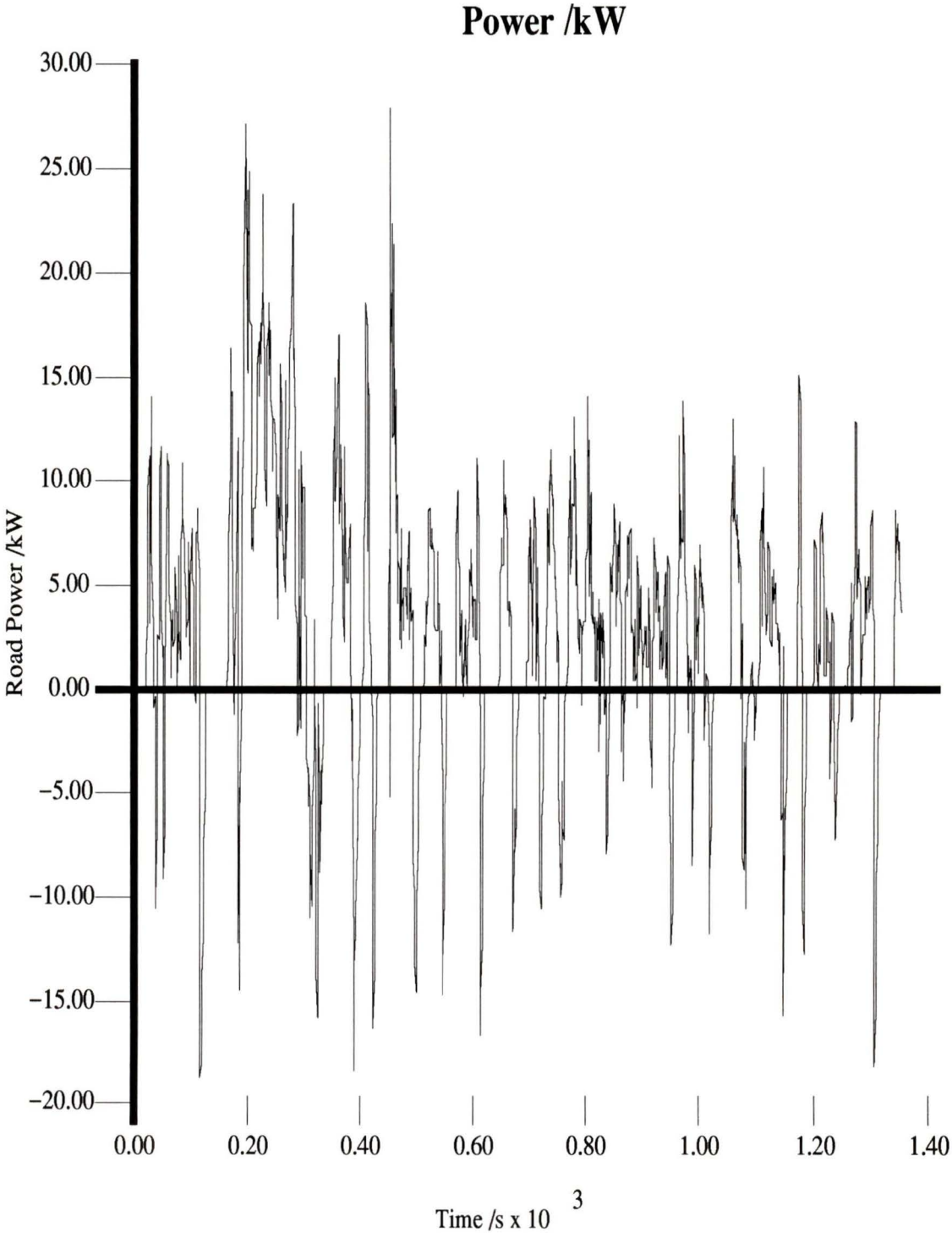

Figure B.3: Road power to the vehicle wheels versus time for an average vehicle undergoing the UDDS.

Appendix C

Fuel Cell System Simulations

The following pages contain the fuel cell system simulation programs (in Pascal), including the data and output files in the following order:

Methanol Pathway

1. Program listing
2. Output

Liquid Hydrogen Pathway

1. Program listing
2. Output

Compressed Hydrogen Pathway

1. Program listing
2. Output

The data input consists of the second–by–second load requirements, as described in Appendix B, for both driving schedules. Each program was run using both the FTP schedule and UDDS schedule, and the results were averaged.

```
program fc (input,output);

{Methanol, fuel cell, auxiliary power, work and heat
produced, requires duty cycle power as input}

const R = 8.314;
To = 298.15;
h2wt = 2.0148;
h2owt = 18.0142;
ch3ohwt = 32.04;
h2prod = 2.985;
cpair = 1.005;
kair = 1.4;
airwt = 28.632461;
mfon2 = 0.7567;
        mfoo2 = 0.2035;
        mfoh2o = 0.0303;
        mfoar = 0.0092;
        mfoco2 = 0.0003;
videal = 1.23;
dhevap = 41.55;
area = 0.25;
nn2 = 2.7888;
no2 = 0.25;
nh2o = 1.11167;
nar = 0.0339;
nco2 = 0.0011;
h2exergy = 238.167; {h2 total exergy at 3 bar, 80 C }
meff = 0.90; {assumed motor efficiency }
ceff = 0.96; {assumed controller efficiency }
ncell = 100; {cell stack size                }

var eff: real;
```

```
vpercell: real;
powerpercell: real;
powerdens: real;
current: real;
ndoth2: real;
ndoto2: real;
ndoth2o: real;
grossheat: real;
netheat: real;
circwatermflow: real;
auxpower: real;
netpower: real;
grosspower: real;
vtotal: real;
gpwrguess: real;
emisex: real;
ntot: real;
dist: real; {distance covered in Test.Proc}

i,j,k: integer;
n: integer;
toth2: real;
dummy: real;
waux: real;
wtot: real;
wideal: real;


procedure findcellvolts(powerdens:real;
var vpercell:real);

{this procedure crudely finds the volts per cell from the curve}
```

```
begin {findcellvolts}

if (powerdens < 0.092) then begin
writeln('You need a smaller stack');
vpercell := 0.95;
end; {if}

if (powerdens >= 0.092) and (powerdens < 0.275) then
vpercell := (powerdens - 0.092)/(0.275 - 0.092) * (0.89 - 0.92) + 0.92;

if (powerdens >= 0.275) and (powerdens < 0.400) then
vpercell := (powerdens - 0.275)/(0.400 - 0.275) * (0.84 - 0.89) + 0.89;

if (powerdens >= 0.400) and (powerdens < 0.800) then
vpercell := (powerdens - 0.400)/(0.800 - 0.400) * (0.78 - 0.84) + 0.84;

if (powerdens >= 0.800) and (powerdens < 1.100) then
vpercell := (powerdens - 0.800)/(1.100 - 0.800) * (0.73 - 0.78) + 0.78;

if (powerdens >= 1.100) and (powerdens < 1.350) then
vpercell := (powerdens - 1.100)/(1.350 - 1.100) * (0.68 - 0.73) + 0.73;

if (powerdens >= 1.350) and (powerdens < 1.575) then
vpercell := (powerdens - 1.350)/(1.575 - 1.350) * (0.63 - 0.68) + 0.68;

if (powerdens >= 1.575) and (powerdens < 1.750) then
vpercell := (powerdens - 1.575)/(1.750 - 1.575) * (0.58 - 0.63) + 0.63;

if (powerdens >= 1.750) and (powerdens < 1.900) then
vpercell := (powerdens - 1.750)/(1.900 - 1.750) * (0.54 - 0.58) + 0.58;

if (powerdens >= 1.900) and (powerdens <= 2.050) then
vpercell := (powerdens - 1.900)/(2.050 - 1.900) * (0.51 - 0.54) + 0.54;

if (powerdens > 2.050) then begin
```

```
writeln('You need a larger stack');
vpercell := 0.5;
end; {if}

end; {procedure findcellvolts}


begin {program}

ntot := nn2 + no2 + nh2o + nco2 + nar;

emisex := R * (To/1000) *(nn2*ln((nn2/ntot)/mfon2) + no2*ln(
(no2/ntot)/mfoo2) + nh2o*ln((nh2o/ntot)/mfoh2o) +
nco2*ln((nco2/ntot)/mfoco2) + nar*ln((nar/ntot)/mfoar));

for k := 1 to 2 do begin

readln(n);

if n = 1877 then
dist := 17.88
else
dist := 12.1;

writeln;
writeln(k:10,n:10,dist:10:3);
writeln;
writeln('Number of cells ',ncell:6:1);
writeln('Assumed power control and conversion efficiency ',100*
meff*ceff:6:2);
{writeln('Road Load Power      Gross Power   ');}
toth2 := 0;
dummy := 0;
waux := 0;
wtot := 0;
```

```
wideal := 0;

for j := 1 to n do begin

readln(netpower);

gpwrguess := netpower;

if netpower <> 2.8 then begin

for i := 1 to 20 do begin
grosspower := gpwrguess;
powerdens := grosspower/(area*ncell);
powerpercell := grosspower/ncell;
findcellvolts(powerdens,vpercell);
vtotal := vpercell * ncell;
current := grosspower*1000/vtotal;
ndoth2 := ncell * current * 0.000010 * 6.24183 /(2 * 6.02338);
ndoto2 := ndoth2 * 0.75;
ndoth2o := ndoth2*(0.11167) + ndoth2;
eff := vpercell/videal;
grossheat := grosspower/eff - grosspower;
if ndoth2o > 0.5484 then
netheat := grossheat - (0.5484 * dhevap)
else
netheat := grossheat - (ndoth2o * dhevap);
circwatermflow := 0.4 * netheat;
auxpower := (ndoto2 * (airwt/mfoo2) * cpair * To * (exp(((kair-1)/kair)
*ln(3)) - 1)/0.7 + ((ndoth2/h2prod) * (ch3ohwt + h2owt) *
9.81 * 40.42) + (circwatermflow * 9.81 * 20))/1000;
gpwrguess := (netpower/meff + auxpower)/ceff;
end {for}
end {part of if}
```

```
else begin
grosspower := 2.8;
powerdens := grosspower/(area*ncell);
powerpercell := grosspower/ncell;
findcellvolts(powerdens,vpercell);
vtotal := vpercell * ncell;
current := grosspower*1000/vtotal;
ndoth2 := ncell * current * 0.000010 * 6.24183 /(2 * 6.02338);
auxpower := (ndoto2 * (airwt/mfoo2) * cpair * To * (exp(((kair-1)/kair)
*ln(3)) - 1)/0.7 + ((ndoth2/h2prod) * (ch3ohwt + h2owt) *
9.81 * 40.42) + (circwatermflow * 9.81 * 20))/1000;

end; {if}

eff := (netpower/meff*ceff)/(ndoth2*h2exergy);
dummy := dummy + eff;

toth2 := toth2 + ndoth2;
wtot := wtot + grosspower;
wideal := wideal + videal*ncell*current/1000;
waux := waux + auxpower/ceff;

end; {for}

writeln;
writeln('Total h2 consumed     : ',toth2*2.0148:9:5,' g');
writeln('Avg. fuel consumption : ',toth2*2.0148/dist:9:5,' g/km');
writeln('Voltage efficiency    : ',(dummy/18.76):8:4);
writeln;
writeln('The gross exergy of emissions is ',emisex*toth2:10:5,' kJ');
writeln('The normalized exergy of emissions is ',(toth2*emisex/dist)
:10:5,' kJ/km');
```

```
writeln;
writeln('EXERGY INPUT          : ',toth2*h2exergy/dist:9:5,' kJ/km');
writeln('EFFECTIVENESS         : ',(wtot-waux)/(toth2*h2exergy):9:5
,' kJ/km');
writeln;
writeln('H2O produced      : ',toth2*h2owt/dist:9:5,' g/km');
writeln('Work produced     : ',wtot/dist:9:5,' kJ/km');
writeln('Auxiliary work    : ',waux/dist:9:5,' kJ/km');
writeln;
writeln('Ideal work              : ',wideal/dist:9:5,' kJ/km');
writeln('Heat produced           : ',(wideal - wtot)/dist:9:5,' kJ/km');

end; {for}

end. {program}

METHANOL OUTPUT
FTP  1      1877    17.880
Number of cells  100.0
Assumed power control and conversion efficiency  86.40

Total h2 consumed      : 169.91474 g
Avg. fuel consumption :   9.50306 g/km
Voltage efficiency     :  66.5329

The gross exergy of emissions is  365.32248 kJ
The normalized exergy of emissions is   20.43191 kJ/km

EXERGY INPUT           : 1123.34510 kJ/km
EFFECTIVENESS          :   0.53522 kJ/km

H2O produced      :  84.96628 g/km
Work produced     : 745.92864 kJ/km
Auxiliary work    : 144.69694 kJ/km
```

```
Ideal work              : 1119.68289 kJ/km
Heat produced           : 373.75426 kJ/km

UDDS     2      1352    12.100


Number of cells  100.0
Assumed power control and conversion efficiency  86.40

Total h2 consumed      : 110.67843 g
Avg. fuel consumption :   9.14698 g/km
Voltage efficiency     :  48.4195

The gross exergy of emissions is  237.96238 kJ
The normalized exergy of emissions is   19.66631 kJ/km

EXERGY INPUT           : 1081.25280 kJ/km
EFFECTIVENESS          :   0.54359 kJ/km

H2O produced      :  81.78255 g/km
Work produced     : 728.37969 kJ/km
Auxiliary work    : 140.62669 kJ/km

Ideal work              : 1077.72782 kJ/km
Heat produced           : 349.34813 kJ/km
```

```
program lh2fc (input,output);

{Hydrogen, liquid, fuel cell, auxiliary power, work and heat
produced, requires duty cycle power as input}

const R = 8.314;
To = 298.15;
h2wt = 2.0148;
h2owt = 18.0142;
cpair = 1.005;
kair = 1.4;
airwt = 28.632461;
mfon2 = 0.7567;
        mfoo2 = 0.2035;
        mfoh2o = 0.0303;
        mfoar = 0.0092;
        mfoco2 = 0.0003;
videal = 1.23;
dhevap = 41.55;
area = 0.25;
nn2 = 2.7888;
no2 = 0.25;
nh2o = 1.11167;
nar = 0.0339;
nco2 = 0.0011;
h2exergy = 264.3; {total exergy, 1.32 bar, 20.57 K}
meff = 0.90; {assumed motor efficiency }
ceff = 0.96; {assumed controller efficiency }
ncell = 100; {cell stack size                }

var eff: real;
vpercell: real;
powerpercell: real;
```

```
powerdens: real;
current: real;
ndoth2: real;
ndoto2: real;
ndoth2o: real;
grossheat: real;
netheat: real;
circwatermflow: real;
auxpower: real;
netpower: real;
grosspower: real;
vtotal: real;
gpwrguess: real;
emisex: real;
ntot: real;
dist: real; {distance covered in Test.Proc}

i,j,k: integer;
n: integer;
toth2: real;
dummy: real;
waux: real;
wtot: real;
wideal: real;


begin {program}

ntot := nn2 + no2 + nh2o + nco2 + nar;

emisex := R * (To/1000) *(nn2*ln((nn2/ntot)/mfon2) + no2*ln(
(no2/ntot)/mfoo2) + nh2o*ln((nh2o/ntot)/mfoh2o) +
nco2*ln((nco2/ntot)/mfoco2) + nar*ln((nar/ntot)/mfoar));
```

```
for k := 1 to 2 do begin

readln(n);

if n = 1877 then
dist := 17.88
else
dist := 12.1;
writeln;
writeln(k:10,n:10,dist:10:3);
writeln;
writeln('Number of cells ',ncell:6:1);
writeln('Assumed power control and conversion efficiency ',100
*meff*ceff:6:2);
{writeln('Road Load Power      Gross Power   ');}
toth2 := 0;
dummy := 0;
waux := 0;
wtot := 0;
wideal := 0;

for j := 1 to n do begin

readln(netpower);

gpwrguess := netpower;

if netpower <> 2.8 then begin

for i := 1 to 12 do begin
grosspower := gpwrguess;
powerdens := grosspower/(area*ncell);
powerpercell := grosspower/ncell;
findcellvolts(powerdens,vpercell);
```

```
vtotal := vpercell * ncell;
current := grosspower*1000/vtotal;
ndoth2 := ncell * current * 0.000010 * 6.24183 /(2 * 6.02338);
ndoto2 := ndoth2 * 0.75;
ndoth2o := ndoth2*(0.11167) + ndoth2;
eff := vpercell/videal;
grossheat := grosspower/eff - grosspower;
if ndoth2o > 0.5484 then
netheat := grossheat - (0.5484 * dhevap)
else
netheat := grossheat - (ndoth2o * dhevap);
circwatermflow := 0.4 * netheat;
auxpower := (ndoto2 * (airwt/mfoo2) * cpair * To * (exp(((kair-1)/kair)
*ln(3)) - 1)/0.7 + (ndoth2 * h2wt * 9.81 * 5) +
(circwatermflow * 9.81 * 20)*0.88)/1000;
gpwrguess := (netpower/meff + auxpower)/ceff;
end {for}
end {part of if}
else begin
grosspower := 2.8;
powerdens := grosspower/(area*ncell);
powerpercell := grosspower/ncell;
findcellvolts(powerdens,vpercell);
vtotal := vpercell * ncell;
current := grosspower*1000/vtotal;
ndoth2 := ncell * current * 0.000010 * 6.24183 /(2 * 6.02338);
auxpower := (ndoto2 * (airwt/mfoo2) * cpair * To * (exp(((kair-1)/kair)
*ln(3)) - 1)/0.7 + (ndoth2 * h2wt * 9.81 * 5) +
(circwatermflow * 9.81 * 20)*0.88)/1000;

end; {if}
```

```
eff := (netpower/meff*ceff)/(ndoth2*h2exergy);
dummy := dummy + eff;

toth2 := toth2 + ndoth2;
wtot := wtot + grosspower;
wideal := wideal + videal*ncell*current/1000;
waux := waux + auxpower/ceff;
{writeln(netpower:10:4,' kW',gpwrguess:10:4,' kW');}

end; {for}

writeln;
writeln('Total h2 consumed     : ',toth2*2.0148:9:5,' g');
writeln('Avg. fuel consumption : ',toth2*2.0148/dist:9:5,' g/km');
writeln('Voltage efficiency    : ',(dummy/18.76):8:4);
writeln;
writeln('The gross exergy of emissions is ',emisex*toth2:10:5,' kJ');
writeln('The normalized exergy of emissions is ',(toth2*emisex/dist)
:10:5,' kJ/km');
writeln;
writeln('EXERGY INPUT          : ',toth2*h2exergy/dist:9:5,' kJ/km');
writeln('EFFECTIVENESS         : ',(wtot-waux)/(toth2*h2exergy):9:5
,' kJ/km');
writeln;
writeln('H2O produced     : ',toth2*h2owt/dist:9:5,' g/km');
writeln('Work produced    : ',wtot/dist:9:5,' kJ/km');
writeln('Auxiliary work   : ',waux/dist:9:5,' kJ/km');
writeln;
writeln('Ideal work             : ',wideal/dist:9:5,' kJ/km');
writeln('Heat produced          : ',(wideal - wtot)/dist:9:5,' kJ/km');
end; {for}
```

```
end. {program}

LIQUID HYDROGEN
FTP
         1      1877    17.880

Number of cells  100.0
Assumed power control and conversion efficiency  86.40

Total h2 consumed     : 160.30964 g
Avg. fuel consumption :   8.96586 g/km
Voltage efficiency    :  61.3248

The gross exergy of emissions is  344.67118 kJ
The normalized exergy of emissions is   19.27691 kJ/km

EXERGY INPUT          : 1176.13546 kJ/km
EFFECTIVENESS         :   0.51801 kJ/km

H2O produced     :  80.16322 g/km
Work produced    : 712.36584 kJ/km
Auxiliary work   : 103.11593 kJ/km

Ideal work             : 1056.38838 kJ/km
Heat produced          : 344.02253 kJ/km

UDDS     2      1352    12.100

Number of cells  100.0
Assumed power control and conversion efficiency  86.40

Total h2 consumed     : 104.87277 g
Avg. fuel consumption :   8.66717 g/km
Voltage efficiency    :  44.5749
```

```
The gross exergy of emissions is  225.48001 kJ
The normalized exergy of emissions is   18.63471 kJ/km

EXERGY INPUT          : 1136.95317 kJ/km
EFFECTIVENESS         :   0.52465 kJ/km

H2O produced     :  77.49263 g/km
Work produced    : 697.45811 kJ/km
Auxiliary work   : 100.95071 kJ/km

Ideal work             : 1021.19539 kJ/km
Heat produced          : 323.73728 kJ/km
```

```
program ch2fc (input,output);

{Compressed hydrogen, fuel cell, auxiliary power, work and heat
produced, requires duty cycle power as input}

const R = 8.314;
To = 298.15;
h2wt = 2.0148;
h2owt = 18.0142;
ch3ohwt = 32.04;
h2prod = 2.985;
cpair = 1.005;
kair = 1.4;
airwt = 28.632461;
mfon2 = 0.7567;
        mfoo2 = 0.2035;
        mfoh2o = 0.0303;
        mfoar = 0.0092;
        mfoco2 = 0.0003;
videal = 1.23;
dhevap = 41.55;
area = 0.25;
nn2 = 2.7888;
no2 = 0.25;
nh2o = 1.11167;
nar = 0.0339;
nco2 = 0.0011;
h2exergy = 250.7; {h2 total exergy, 311 bar, 25 C }
meff = 0.90; {assumed motor efficiency }
ceff = 0.96; {assumed controller efficiency }
ncell = 100; {cell stack size                }

var eff: real;
```

```
vpercell: real;
powerpercell: real;
powerdens: real;
current: real;
ndoth2: real;
ndoto2: real;
ndoth2o: real;
grossheat: real;
netheat: real;
circwatermflow: real;
auxpower: real;
netpower: real;
grosspower: real;
vtotal: real;
gpwrguess: real;
emisex: real;
ntot: real;
dist: real; {distance covered in Test.Proc}

i,j,k: integer;
n: integer;
toth2: real;
dummy: real;
waux: real;
wtot: real;
wideal: real;

begin {program}

ntot := nn2 + no2 + nh2o + nco2 + nar;

emisex := R * (To/1000) *(nn2*ln((nn2/ntot)/mfon2) + no2*ln(
(no2/ntot)/mfoo2) + nh2o*ln((nh2o/ntot)/mfoh2o) +
```

```
nco2*ln((nco2/ntot)/mfoco2) + nar*ln((nar/ntot)/mfoar));

for k := 1 to 2 do begin

readln(n);
if n = 1877 then
dist := 17.88
else
dist := 12.1;
writeln;
writeln(k:10,n:10,dist:10:3);
writeln;
writeln('Number of cells ',ncell:6:1);
writeln('Assumed power control and conversion efficiency ',100
*meff*ceff:6:2);
{writeln('Road Load Power      Gross Power   ');}
toth2 := 0;
dummy := 0;
waux := 0;
wtot := 0;
wideal := 0;

for j := 1 to n do begin

readln(netpower);

gpwrguess := netpower;

if netpower <> 2.8 then begin

for i := 1 to 12 do begin
grosspower := gpwrguess;
powerdens := grosspower/(area*ncell);
powerpercell := grosspower/ncell;
findcellvolts(powerdens,vpercell);
```

```
vtotal := vpercell * ncell;
current := grosspower*1000/vtotal;
ndoth2 := ncell * current * 0.000010 * 6.24183 /(2 * 6.02338);
ndoto2 := ndoth2 * 0.75;
ndoth2o := ndoth2*(0.11167) + ndoth2;
eff := vpercell/videal;
grossheat := grosspower/eff - grosspower;
if ndoth2o > 0.5484 then
netheat := grossheat - (0.5484 * dhevap)
else
netheat := grossheat - (ndoth2o * dhevap);
circwatermflow := 0.4 * netheat;
auxpower := (ndoto2 * (airwt/mfoo2) * cpair * To * (exp(((kair-1)/kair)
*ln(3)) - 1)/0.7 + (circwatermflow * 9.81 * 20)*1.25)/1000;
gpwrguess := (netpower/meff + auxpower)/ceff;
end {for}
end {part of if}
else begin
grosspower := 2.8;
powerdens := grosspower/(area*ncell);
powerpercell := grosspower/ncell;
findcellvolts(powerdens,vpercell);
vtotal := vpercell * ncell;
current := grosspower*1000/vtotal;
ndoth2 := ncell * current * 0.000010 * 6.24183 /(2 * 6.02338);
auxpower := (ndoto2 * (airwt/mfoo2) * cpair * To * (exp(((kair-1)/kair)
*ln(3)) - 1)/0.7 + (circwatermflow * 9.81 * 20)*1.25)/1000;

end; {if}

eff := (netpower/meff*ceff)/(ndoth2*h2exergy);
```

```
dummy := dummy + eff;

toth2 := toth2 + ndoth2;
wtot := wtot + grosspower;
wideal := wideal + videal*ncell*current/1000;
waux := waux + auxpower/ceff;
{writeln(netpower:10:4,' kW',gpwrguess:10:4,' kW');}

end; {for}

writeln;
writeln('Total h2 consumed     : ',toth2*2.0148:9:5,' g');
writeln('Avg. fuel consumption : ',toth2*2.0148/dist:9:5,' g/km');
writeln('Voltage efficiency    : ',(dummy/18.76):8:4);
writeln;
writeln('The gross exergy of emissions is ',emisex*toth2:10:5,' kJ');
writeln('The normalized exergy of emissions is ',(toth2*emisex/dist)
:10:5,' kJ/km');
writeln;
writeln('EXERGY INPUT          : ',toth2*h2exergy/dist:9:5,' kJ/km');
writeln('EFFECTIVENESS         : ',(wtot-waux)/(toth2*h2exergy):9:5
,' kJ/km');
writeln;
writeln('H2O produced     : ',toth2*h2owt/dist:9:5,' g/km');
writeln('Work produced    : ',wtot/dist:9:5,' kJ/km');
writeln('Auxiliary work   : ',waux/dist:9:5,' kJ/km');
writeln;
writeln('Ideal work            : ',wideal/dist:9:5,' kJ/km');
writeln('Heat produced         : ',(wideal - wtot)/dist:9:5,' kJ/km');
end; {for}

end. {program}
```

COMPRESSED HYDROGEN
FTP
1 1877 17.880

Number of cells 100.0
Assumed power control and conversion efficiency 86.40

Total h2 consumed : 161.60801 g
Avg. fuel consumption : 9.03848 g/km
Voltage efficiency : 64.4970

The gross exergy of emissions is 347.46271 kJ
The normalized exergy of emissions is 19.43304 kJ/km

EXERGY INPUT : 1124.65095 kJ/km
EFFECTIVENESS : 0.54083 kJ/km

H2O produced : 80.81247 g/km
Work produced : 716.69736 kJ/km
Auxiliary work : 108.45324 kJ/km

Ideal work : 1064.94421 kJ/km
Heat produced : 348.24685 kJ/km

UDDS 2 1352 12.100

Number of cells 100.0
Assumed power control and conversion efficiency 86.40

Total h2 consumed : 105.61592 g
Avg. fuel consumption : 8.72859 g/km
Voltage efficiency : 46.8927

The gross exergy of emissions is 227.07781 kJ
The normalized exergy of emissions is 18.76676 kJ/km

```
EXERGY INPUT          : 1086.09145 kJ/km
EFFECTIVENESS         :   0.54823 kJ/km

H2O produced     :  78.04176 g/km
Work produced    : 701.22395 kJ/km
Auxiliary work   : 105.79306 kJ/km

Ideal work            : 1028.43180 kJ/km
Heat produced         : 327.20785 kJ/km
```

VITA

Surname: Crane Given Names: Patricia
Place of Birth: Toronto, Ontario Date of Birth: 64/12/11

Educational Institutions Attended:

University of Victoria	1989 to 1991
University of Toronto	1983 to 1988

Degrees Awarded:

M.A.Sc.	University of Victoria	1991
B.A.Sc.	University of Toronto	1988

Publications:

1. *Exergy of Emissions as a Mearusre of Potential for Environmental Impact.* P. Crane, D. S. Scott, M. A. Rosen. Hydrogen Energy Progress VIII, Proceedings of the 8th World Hydrogen Energy Conference, Pergamon Press, July 1990.

2. *An Exergy Approach to Measurement of Environmental Impact in Terms of Service Provided.* P. Crane, D. S. Scott. Presented at the Air and Waste Management Association 84th Annual Meeting, Vancouver, June 1991.

3. *Comparison of Exergy of Emissions From Two Energy Conversion Technologies, Considering Potential for Environmental Impact.* P. Crane, D. S. Scott, M. A. Rosen. Accepted for Publication in International Journal of Energy · Environment · Economics, Pergamon Press, April, 1991.

PARTIAL COPYRIGHT LICENSE

I hereby grant the right to lend my thesis to users of the University of Victoria Library, and to make single copies only for such users or in response to a request from the Library of any other university, or similar institution, on its behalf or for one of its users. I further agree that permission for extensive copying of this thesis for scholarly purposes may be granted by me or a member of the University designated by me. It is understood that copying or publication of this thesis for financial gain shall not be allowed without my written permission.

Title of Thesis: An Exergy Perspective on Selecting Technical Pathways by Which Methane Can Provide Transportation Services.

Author [redacted]

(Signature)

PATRICIA CRANE

(Name in Block Letters)

JULY 23, 1991

(Date)